Published by Institute of Physics Publishing for SISSA

Received: *June 23, 2005*
Revised: *October 31, 2005*
Accepted: *November 29, 2005*
Published: *January 12, 2006*

On the integrability of Wilson loops in $AdS_5 \times S^5$: some periodic ansatze

Nadav Drukker

The Niels Bohr Institute, Copenhagen University
Blegdamsvej 17, DK-2100 Copenhagen, Denmark
E-mail: drukker@nbi.dk

Bartomeu Fiol

Institute for Theoretical Physics, University of Amsterdam
1018 XE Amsterdam, the Netherlands
E-mail: bfiol@science.uva.nl

Abstract: Wilson loops are calculated within the AdS/CFT correspondence by finding a classical solution to the string equations of motion in $AdS_5 \times S^5$ and evaluating its action. An important fact is that this σ-model used to evaluate the Wilson loops is integrable, a feature that has gained relevance through the study of spinning strings carrying large quantum numbers and spin-chains. We apply the same techniques used to solve the equations for spinning strings to find the minimal surfaces describing a wide class of Wilson loops. We focus on different cases with periodic boundary conditions on the AdS_5 and S^5 factors and find a rich array of solutions. We examine the different phases that appear in the problem and comment on the applicability of integrability to the general problem.

Keywords: Integrable Field Theories, AdS-CFT Correspondence.

JHEP01(2006)056

Contents

JHEP01(2006)056

1. Introduction

Wilson loops are some of the most interesting observables in non-abelian gauge theories. In addition to their paramount role as the order parameter for confinement, they constitute a large class of non-local gauge invariant observables. In the AdS/CFT [1] correspondence they are realized in a very suggestive way: the expectation value of the Wilson loop is given by the string partition function with appropriate boundary conditions. The superstring in $AdS_5 \times S^5$ bound by the loop represents the Wilson loop in the same way the QCD string should give the area-law of a confining gauge theory.

In practical applications one uses $AdS_5 \times S^5$ to evaluate the Wilson loop at large N and 't Hooft coupling $\lambda = g_{YM}^2 N$. On the string theory side this translates to weak string coupling $g_s = \lambda/(4\pi N)$ and large string tension (or large AdS_5 and S^5 radii L), since $\lambda = L^4/\alpha'^2$. In this limit the string calculation reduces to finding the minimal surface with appropriate boundary conditions and evaluating its action.

Despite their importance, the study of Wilson loops in the AdS/CFT correspondence hasn't benefited from the same impetus as that of local gauge theory operators. In particular, the exciting discovery of integrable structures on both sides of the duality has been so far applied only to local operators. One of the main purposes of the present work is to extend the tools of integrability also to operators that are non-local on the gauge theory.

In order to place this work in perspective, it is useful to remind ourselves of the status of classical integrability in AdS/CFT, mostly on the string theory side of the duality (for reviews on the impressive body of work on integrability on the gauge theory side, see e.g. [2]). Integrability of two-dimensional non-linear sigma models has been known for many years [3]. The world-sheet description of string theory on $AdS_5 \times S^5$ is given by two non-linear sigma models, related by the Virasoro constraints [4]. In [5] it was observed that the presence of Virasoro constraints doesn't affect the construction of currents, so the full bosonic sector of the world-sheet description is integrable. It was later shown in [6] that classical integrability extends to the fermionic sector.

These non-linear sigma models can be simplified by considering particular ansatze. A prime example are the spinning string solutions [7, 8]. In the world-sheet this ansatz reduces the full non-lineal σ-model to a much simpler $1d$ integrable system [9, 10].

The simple but far-reaching observation, which is the starting point of this work, is that locally supersymmetric Wilson loops are calculated within the AdS/CFT correspondence using the same integrable classical σ-model. While for the local operators the classical description in terms of string solutions is valid only at large quantum numbers, the Wilson loops we consider may always be studied by semiclassical methods. Thus the integrability of the σ-model should be utilized to evaluate those non-local observables.

In this paper we perform some concrete calculations of Wilson loop observables by considering periodic ansatze similar to those of the rotating strings [9, 10]. The resulting surfaces will evaluate Wilson loops whose contours are symmetric, like straight lines and circles, and with periodic couplings to the scalar fields. Those will include as particular cases many of the Wilson loops evaluated previously within the AdS/CFT framework.

JHEP01(2006)056

Note that we will study the Wilson loops only on the string side of the duality. For the local operators, an integrable structure was also found in the gauge theory at weak coupling in terms of the Bethe ansatz solution of spin-chains [11]. In certain cases the correspondence with spinning strings allows to calculate conformal dimensions reliably on both sides and compare the results, which exhibit remarkable agreement. But the statement about integrability of the σ-model does not require this agreement between strong and weak coupling. In fact, in the examples we study, we generally did not find a simple agreement between the gauge theory calculation and the one in $AdS_5 \times S^5$, so we are focusing exclusively on the latter.

One of the most salient aspects of the present work is that the geometric data that define the Wilson loop operator (e.g. distance between parallel lines, ratio of radii), is not all encoded in a straight-forward manner in terms of the parameters and the integrals of motion of the $1d$ integrable model. In the general case we will see that they are related by equations that can't be easily inverted, and require numerical analysis. More than that, there is not even a one to one correspondence and generically there are many classical solutions to the σ-model for the same boundary conditions.

As stated above, in this paper we will focus on the string theory side of the duality, and already there we will find some very confusing phenomena. We will comment on some of the difficulties in the comparison to the weakly coupled gauge theory in the final section.

It is worth mentioning the one case where there is good agreement between the gauge theory and string results, which is the circular Wilson loop (with simplest coupling to the scalars) [12, 13]. In that case summing up the perturbative series (assuming no interactions) leads exactly to the string result including all non-planar corrections [14 – 16]. The agreement seems to hold for both the expectation value of the Wilson loop, as well as the correlation function of the Wilson loop with some local operators [17, 18].

The paper is organized as follows. In the rest of the introduction we present the types of Wilson loops we will be studying. Then we will set up the σ-model calculation. In section 2 we look at the S^5 part of the equations and solve them for periodic motion. We write explicitly the solutions for motions in S^1, S^2 and S^3 subspaces which we utilize later. In the following section we do the same for the AdS_5 part of the action, solving it for general periodic motions and then concentrating on solutions within AdS_2 and AdS_3 subspaces. Those include a line, circle, parallel lines and concentric circles.

In section 4 we put this all together into full solutions in $AdS_5 \times S^5$. We start with solutions in AdS_2, which are just the straight line and the circle. This is the one case where there is an explicit calculation relating the string results to the gauge theory, and we review it there. We then discuss solutions within $AdS_3 \times S^1$, which include two lines or concentric circles that may be separated on the S^5. The case of the lines was already studied in the original papers [19, 20] and the circles (without the S^1 dependence) were studied before in [21, 22].

The next solutions we consider live in an $AdS_2 \times S^2$ subspace of $AdS_5 \times S_5$. They correspond to a line or circle with periodic motion inside an S^2, generalizing solutions presented in [23, 24]. Finally we study the periodic motions inside an $AdS_3 \times S^3$ subspace

JHEP01(2006)056

(the simplest of those was discussed in [24]). Those are parallel lines and concentric circles that also rotate on an S^2, and they exhibit very rich phenomena. We find at least four types of classical solutions and describe the phase transitions between them.

We end with a discussion on the results and some general speculations on the integrability of Wilson loop operators.

1.1 The observables

The (locally) supersymmetric Wilson loops in $\mathcal{N} = 4$ supersymmetric Yang-Mills include a coupling to both the gauge field A_μ and the scalars Φ_i. The general observable is

$$W = \frac{1}{N} \operatorname{Tr} \mathcal{P} \exp \left[i \int \left(A_\mu \dot{x}^\mu(t) + i|\dot{x}(t)| \Theta^i(t) \Phi_i \right) dt \right] . \tag{1.1}$$

Here x^μ describes the curve in space and Θ^i are unit vectors in $\mathbb{R}^6$. More general operators will include also couplings to the fermionic fields, but we will study the bosonic operators only.

The fact that the magnitude of the coupling to the scalar is equal to the coupling to the gauge field is crucial to guarantee the existence of a classical solution to the equations of motion. It is actually not know how to evaluate Wilson loops not obeying this constraint. Another point to note is the extra factor of i in front of the scalar term. This shows up upon Wick rotation to the Euclidean theory (which we study here), and is also natural for spatial loops in the lorentzian case.

We will be interested in loops following circular or straight paths in space. First we shall look at the infinite line

$$x^1 = t \, , \tag{1.2}$$

and then at the circle

$$x^1 = R \cos kt \, , \qquad x^2 = R \sin kt \, . \tag{1.3}$$

In both cases we will label the length of the line by T, so $0 < t < T$. In the first case T will be a cutoff on the diverging length, and in the second case $T = 2\pi$. Then the integer k describes the number of times the loop wraps the circle. We will also consider the correlator of two of those operators.

While we will not study those cases in detail, we will also solve the equations of motion (implicitly) for loop with rotation in two planes

$$\begin{aligned} x^1 &= R_1 \cos k_1 t \, , & x^2 &= R_1 \sin k_1 t \, , \\ x^3 &= R_2 \sin k_2 t \, , & x^4 &= R_2 \sin k_2 t \, , \end{aligned} \tag{1.4}$$

with $k_1 \neq k_2$ two integers. There is also the helical Wilson loop, where one of the circles is replaced with a straight line (R_2 taken to be infinite)

$$x^1 = R \cos k_1 t \, , \qquad x^2 = R \sin k_1 t \, , \qquad x^3 = t \, , \tag{1.5}$$

Our general ansatz will address the possibility of turning on as many as all six of the scalar fields in the following way

$$\begin{aligned}\Theta^1(t) + i\Theta^2(t) &= \sin\theta\, e^{i(m_1 t+\varphi_1)}\,,\\ \Theta^3(t) + i\Theta^4(t) &= \cos\theta\sin\psi\, e^{i(m_2 t+\varphi_2)}\,,\\ \Theta^5(t) + i\Theta^6(t) &= \cos\theta\cos\psi\, e^{i(m_3 t+\varphi_3)}\,.\end{aligned} \tag{1.6}$$

In the example we study in detail we will turn on at most three scalars, i.e. the above ansatz with $m_2 = m_3 = \cos\psi = \varphi_2 = 0$

If $\theta = \pi/2$ and $m_1 = 0$ there is only a coupling to Θ^1, which is the case considered most often. But some more complicated couplings to the sphere were considered in the past, for example, $\theta = \pi/2$ and $m_1 = k$ is the supersymmetric loop studied in [23].

The map from the gauge theory to $AdS_5 \times S^5$ is the following: the Wilson loop will be described by a minimal surface that will follow the contour x^μ on the boundary, and the derivative normal to the boundary of the surface of the radial coordinate y and angular coordinates, combined together into a six-vector, is proportional to Θ^i, so

$$\partial_\sigma(y^i) \propto \Theta^i\,. \tag{1.7}$$

In all the cases we study the surfaces are smooth, which implies that $\Theta^i(t)$ will be equal to the boundary values of the S^5 coordinates.

1.2 The σ-model

The bosonic part of the action of a string in $AdS_5 \times S^5$ is a standard σ-model

$$\frac{1}{4\pi\alpha'}\int d\tau\, d\sigma\, \sqrt{g}\, g^{\alpha\beta}\partial_\alpha X^M \partial_\beta X^N G_{MN}\,. \tag{1.8}$$

Here G_{MN} is the target space metric for $AdS_5 \times S^5$ each with curvature radius L. By the AdS/CFT correspondence it is related to the 't Hooft coupling $\lambda = g_{YM}^2 N$ of the dual gauge theory and the string scale by $L^4 = \lambda\alpha'^2$.

The ansatz we consider factorizes into an AdS_5 part and an S^5 part, yielding independent equations of motion for the respective variables. These two parts of the ansatz are related only in two ways. One is the range of the world-sheet coordinates, which clearly has to agree, and the other are the Virasoro constraints. Therefore, it makes sense to consider separately the S^5 and AdS_5 parts of the ansatz.

The Virasoro constraints are the vanishing of the stress-energy tensor which in the conformal gauge is given by

$$T_{\sigma\sigma} = -T_{\tau\tau} = \frac{1}{8\pi\alpha'}\left[\partial_\sigma X^M \partial_\sigma X^N - \partial_\tau X^M \partial_\tau X^N\right] G_{MN} = 0\,, \tag{1.9}$$

$$T_{\sigma\tau} = T_{\tau\sigma} = \frac{1}{4\pi\alpha'}\,\partial_\sigma X^M \partial_\tau X^N G_{MN} = 0\,. \tag{1.10}$$

Since our space has a product structure we can decompose the stress-energy tensor into independent contributions from AdS_5 and from S^5

$$T_{\alpha\beta} = T_{\alpha\beta}^{AdS_5} + T_{\alpha\beta}^{S^5}\,. \tag{1.11}$$

The Virasoro constraints are then

$$T^{AdS_5}_{\alpha\beta} + T^{S^5}_{\alpha\beta} = 0\,. \tag{1.12}$$

For notational simplicity we label $a^2 \equiv 8\pi\alpha' T^{S^5}_{\sigma\sigma}/L^2$, and in AdS_5 this parameter serves a role similar to a mass term coming from the Kaluza-Klein reduction on the sphere.

Since the stress-energy tensors of both σ-models are separately conserved, we have

$$\partial_\sigma T^{S^5}_{\sigma\sigma} + \partial_\tau T^{S^5}_{\tau\sigma} = 0 \tag{1.13}$$

and a similar equation for AdS_5. In the ansatze we will use below, $T^{S^5}_{\sigma\tau}$ is always constant (actually zero for the examples we consider in more detail), so it follows that a^2 is constant. Note that a^2 may be either positive or negative.

2. The S^5 ansatz

We start by studying the σ-model on S^5. The standard metric on the sphere is

$$ds^2_{S^5} = L^2\left(d\theta^2 + \sin^2\theta d\varphi_1^2 + \cos^2\theta\left(d\psi^2 + \sin^2\psi d\varphi_2^2 + \cos^2\psi d\varphi_3^2\right)\right). \tag{2.1}$$

Following [9, 25], we use embedding coordinates in flat $\mathbb{R}^6$ by defining three radial coordinates

$$\rho_1 = \sin\theta\,, \qquad \rho_2 = \cos\theta\sin\psi\,, \qquad \rho_3 = \cos\theta\cos\psi\,, \tag{2.2}$$

which clearly satisfy $\sum \rho_i^2 = 1$, which we impose through the inclusion of a Lagrange multiplier Λ. The S^5 part of the action is

$$\mathcal{S}_{S^5} = \frac{L^2}{4\pi\alpha'}\int d\sigma\, d\tau\left[\sum_{i=1}^{3}\left(\rho_i'^2 + \dot\rho_i^2 + \rho_i^2(\varphi_i'^2 + \dot\varphi_i^2)\right) + \Lambda\left(\sum_{i=1}^{3}\rho_i^2 - 1\right)\right]. \tag{2.3}$$

We are interested in the ansatz[1]

$$\rho_i = \rho_i(\sigma)\,, \qquad \varphi_i = m_i\tau + \beta_i(\sigma)\,, \tag{2.4}$$

where m_i are arbitrary constants (which have to be integers for a compact world-sheet). One can check that this ansatz solves the equations of motion and it leads to the action

$$\mathcal{S}_{S^5} = \frac{L^2}{4\pi\alpha'}\int d\sigma\, d\tau\left[\sum_{i=1}^{3}\left(\rho_i'^2 + \rho_i^2(\beta_i'^2 + m_i^2)\right) + \Lambda\left(\sum_{i=1}^{3}\rho_i^2 - 1\right)\right]. \tag{2.5}$$

The τ integration just gives an overall factor of the length of the Wilson line, T, thus we are left with a one-dimensional problem, the Neumann-Rosochatius system, a particular case of the $n = 6$ Neumann system. Clearly β_i are cyclic, with conserved momenta π_i, so

$$\beta_i' = \frac{\pi_i}{\rho_i^2}\,. \tag{2.6}$$

[1] Compared to the spinning string ansatz the coordinates σ and τ are reversed, since we consider the direction along the curve at the boundary to be the (Euclidean) time direction.

The other equations of motion are

$$\rho_i'' = \frac{\pi_i^2}{\rho_i^3} + \rho_i(m_i^2 + \Lambda)\,, \tag{2.7}$$

The Neumann-Rosochatius system is integrable, and it's easy to check that the following three quantities

$$I_i = \rho_i^2 - \sum_{j\neq i} \frac{1}{m_i^2 - m_j^2}\left((\rho_i\rho_j' - \rho_j\rho_i')^2 + \frac{\pi_i^2}{\rho_i^2}\rho_j^2 + \frac{\pi_j^2}{\rho_j^2}\rho_i^2\right), \tag{2.8}$$

with $i = 1,\ 2,\ 3$ are constants of motion. They are not independent, but satisfy $I_1+I_2+I_3 = 1$. Another identity relates them to the S^5 contribution to the stress-energy tensor

$$\frac{8\pi\alpha'}{L^2}\,T^{S^5}_{\sigma\sigma} = a^2 = \sum_{i=1}^{3}\left(\pi_i^2 - m_i^2 I_i\right) = \sum_{i=1}^{3}\left(\rho_i'^2 + \frac{\pi_i^2}{\rho_i^2} - \rho_i^2 m_i^2\right). \tag{2.9}$$

The off-diagonal contribution to the stress-energy tensor, $T_{\sigma\tau} = (L^2/4\pi\alpha')\sum m_i\pi_i$ is also a constant.

When evaluating the classical action of our solutions we may use this conserved quantity to replace the potential terms with the kinetic terms

$$\mathcal{S}_{S^5} = \frac{\sqrt{\lambda}}{4\pi}\int d\sigma\, d\tau\left[2\sum_{i=1}^{3} m_i^2\rho_i^2 + a^2\right] = 2\mathcal{S}^{\rm kinetic}_{S^5} + \frac{\sqrt{\lambda}}{4\pi}a^2\delta\sigma T\,. \tag{2.10}$$

T is the range of the coordinate τ, or the length of the Wilson loop, and $\delta\sigma$ is the range of the σ coordinate. So the second term on the right hand side is proportional to the volume of the world-sheet. Due to the Virasoro constraint, it will be canceled by a similar term from the AdS_5 part of the σ-model, the total classical action will be just twice the sum of the kinetic terms on both sides.

Finally, it is worth noticing that since the integrand in (2.5) is positive, the S^5 contribution to the full action is positive, and the same is true for the kinetic term alone.

2.1 S^1 ansatz

We look now at specific examples, starting with an ansatz that turns on only a single angle φ_1.

In order for the other angles to be constants we have to take $\rho_1 = 1$, or $\theta = \pi/2$ and consequently $\rho_2 = \rho_3 = 0$. To turn on this angle in the framework of our general ansatz we should take only $\pi_1 \neq 0$ while $\pi_2 = \pi_3 = 0$. We also set all three $m_i = 0$.

There is another possibility, where we turn on m_1 instead of π_1. This imposes boundary conditions within this S^1 equator of S^5, but as we will see in the next subsection, the resulting minimal surface will generally not stay at $\rho_1 = 1$. The solution will break the symmetry and extend into some other direction, so we treat that case there.

The only equation of motion is $\varphi_1' = \pi_1$, and is solved by $\varphi_1 = \varphi_{1i} + \pi_1\sigma$. The contribution to the stress-energy tensor is proportional to $a^2 = \pi_1^2$, which will feed into the Virasoro constraint equation. The integration constants I_i are not well defined.

This ansatz will be used below when looking at the correlator of two Wilson loops separated in the φ_1 direction as was originally studied in [20]. The boundary conditions specifying φ_1 along each loop, φ_{1i} and φ_{1f}, will fix π_1. The difference in the value of this angle between the two loops is related to the range of the world-sheet variable σ by

$$\delta\varphi_1 = \pm a\delta\sigma\,. \tag{2.11}$$

See section 4.2 below.

The classical action for this solution has no kinetic term, so when combining this ansatz with the AdS_5 part the full action will be given by twice the kinetic term in the AdS_5 action.

2.2 S^2 ansatz

Let us look now at the case when we turn on two of the angles, θ and φ_1, by including a single rotation, $m_1 = m$. Then $\rho_1 = \sin\theta$, $\rho_2 = \cos\theta$, $\rho_3 = 0$. If we take $\pi_i = 0$, the conserved energy (2.9) reads

$$\rho_1'^2 + \rho_2'^2 - m^2\rho_1^2 = \theta'^2 - m^2\sin^2\theta = a^2\,. \tag{2.12}$$

In some cases, like when considering the expectation value of a single Wilson loop the constant is $a^2 = 0$, but in other cases, involving the correlator of two loops, a^2 may be positive or negative. For positive a^2 the angle θ will be a monotonous function of σ. For negative a^2, there will be an extremum for θ at some value θ_m, where $a^2 = -m^2\sin^2\theta_m$.

In the special case when $a = 0$ the solution is very simple

$$\sin\theta = \frac{1}{\cosh m(\pm\sigma + \sigma_i)}\,. \tag{2.13}$$

We take the world-sheet coordinate to start at $\sigma = 0$, where the boundary value of θ fixes σ_i by $\sin\theta_i = 1/\cosh m\sigma_i$. If σ extends to infinity, as will be the case for the single loop, the variable θ will reach the north or south pole of the sphere, depending on the sign choice.

The action in this case is twice the kinetic term

$$\mathcal{S}_{S^5} = 2\mathcal{S}_{S^5}^{\text{kinetic}} = \frac{L^2}{4\pi\alpha'}\int d\tau\, d\sigma\, 2m^2\sin^2\theta = \frac{T\sqrt{\lambda}}{2\pi}\int d\theta\,|\theta'| = \frac{T\sqrt{\lambda}}{2\pi}m|\cos\theta_f - \cos\theta_i|\,. \tag{2.14}$$

Here we discussed two solutions covering the northern or southern hemisphere, but it is also possible to cover the sphere more times. Those extra wrappings are unstable world-sheet instantons, wrapping the sphere at a fixed point inside AdS_5. They can occur anywhere on the world-sheet, but in our symmetric ansatz they can be only at symmetric points. Clearly those will never give the dominant contribution to the action.

For $a^2 > 0$ it is still easy to integrate (2.12) in terms of elliptic integrals of the first kind with argument θ and modulus im/a

$$\sigma + \sigma_i = \pm\frac{1}{a}F\left(\theta\,\middle|\, i\frac{m}{a}\right). \tag{2.15}$$

As we will see in section 3, when $a \neq 0$ the surface describes the correlator of two Wilson loops. Let us take θ_i and θ_f to be the boundary values of θ on the two loops. If the surface starts at $\sigma = 0$ on the first loop, σ_i is fixed by (2.15) with $\theta = \theta_i$. The range of the σ variable is given by

$$\delta\sigma = \frac{1}{a}\left|F\left(\theta_f\middle| i\frac{m}{a}\right) - F\left(\theta_i\middle| i\frac{m}{a}\right)\right|. \tag{2.16}$$

This will have to agree with the AdS_5 part of the ansatz.

We can also write the action in terms of elliptic integrals of the first and second kind. The kinetic part is

$$\begin{aligned} 2\mathcal{S}^{\text{kinetic}}_{S^5} &= \frac{\sqrt{\lambda}}{4\pi}\int d\tau\, d\sigma\, 2m^2\sin^2\theta = \frac{T\sqrt{\lambda}}{2\pi}\int d\theta\, \frac{m^2\sin^2\theta}{|\theta'|} \\ &= \pm\frac{T\sqrt{\lambda}}{2\pi}a\left[E\left(\theta\middle| i\frac{m}{a}\right) - F\left(\theta\middle| i\frac{m}{a}\right)\right]_{\theta_i}^{\theta_f}. \end{aligned} \tag{2.17}$$

The above solutions are technically also valid for $a^2 < 0$, but there are other expressions for the above elliptic integrals that are more suitable for this case

$$\sigma + \sigma_i = \pm\frac{1}{b}F\left(\arccos\frac{\cos\theta}{\cos\theta_m}\middle| i\cot\theta_m\right), \tag{2.18}$$

where we used $b^2 = -a^2$, and $\sin\theta_m = b/m$.

This solution has a turning points at $\theta = \theta_m$ and $\theta = \pi - \theta_m$ where $\sigma + \sigma_i$ will be equal to some integral multiple of the complete elliptic integral. This turning point may, or may not, be on the world-sheet.[2] To describe the solution with the turning point we consider the two branches with positive and negative signs in (2.18). This will have the turning point at $\sigma + \sigma_i = 0$. If we take the solution with only one branch, it will not have a turning point along the world-sheet. In either case the value of σ_i is fixed by plugging in the boundary value θ_i.

The full range of σ is now given by

$$\delta\sigma = \frac{1}{b}\left|F\left(\arccos\frac{\cos\theta_f}{\cos\theta_m}\middle| i\cot\theta_m\right) \pm F\left(\arccos\frac{\cos\theta_i}{\cos\theta_m}\middle| i\cot\theta_m\right)\right|. \tag{2.19}$$

In the case with a turning point we have to take the positive sign, to add the contribution from both branches. The negative sign is taken when there is no turning point along the world-sheet.

Finally, the kinetic part of the action is

$$2\mathcal{S}^{\text{kinetic}}_{S^5} = \frac{T\sqrt{\lambda}}{2\pi}b\left[E\left(\arccos\frac{\cos\theta_f}{\cos\theta_m}\middle| i\cot\theta_m\right) \pm E\left(\arccos\frac{\cos\theta_i}{\cos\theta_m}\middle| i\cot\theta_m\right)\right], \tag{2.20}$$

and the sign is chosen as in (2.19)

[2]There are also solutions with more than one turning point, which combine more than two branches of the solution, but their action will be larger than the others.

A special case of the above solution occurs when $\theta_i = \theta_f = \pi/2$ (and $a^2 < 0$). Then the expression for the range of σ (2.19) involves complete elliptic integrals. While one would expect $\theta_m < \pi/2$, the equations of motion are also solved by a constant $\theta = \pi/2$.

This constant solution is unstable, but as we will see in section 4.4, this case is realized when combined with the AdS_5 part. The maximal values of the complete elliptic integrals is for vanishing modulus, where $K(0) = \pi/2$, so the above ansatz allows only $\delta\sigma < \pi/m$. For a longer world-sheet we need to take the constant solution, which puts no restriction on $\delta\sigma$. The kinetic part of the action in this case is

$$\mathcal{S}^{\text{kinetic}}_{S^5} = \frac{T\sqrt{\lambda}}{2\pi}\, m^2 \delta\sigma\,. \tag{2.21}$$

2.3 S^3 ansatz

We may also consider the case with $\pi_2 \neq 0$ with very small modification. In addition to the two angles that were already turned on, θ and φ_1, this ansatz will include φ_2, but we still assume that $\rho_3 = 0$, or $\psi = \pi/2$. The metric for the three coordinates is

$$ds^2 = d\theta^2 + \sin^2\theta d\varphi_1^2 + \cos^2\theta d\varphi_2^2\,. \tag{2.22}$$

So we are studying periodic motion on S^3.

In terms of $\rho_1 = \sin\theta = \sqrt{1-\rho_2^2}$, the first integral (2.9) reads

$$\rho_1'^2 = a^2 - \pi_2^2 + (m_1^2 - a^2)\rho_1^2 - m_1^2\rho_1^4\,. \tag{2.23}$$

This equation will have real solutions for both positive and negative a^2, but there are some constraints. First we require $|a^2 + m_1^2| \geq 2|m_1\pi_2|$ and in addition, if $a^2 < \pi_2^2$, then $m_1^2 \geq a^2$.

Again this may be integrated in terms of elliptic integrals. For $a^2 > \pi_2^2$ we write

$$\sigma + \sigma_i = \pm\frac{\rho_+}{\sqrt{a^2-\pi_2^2}} F\left(\arcsin\frac{\rho_1}{\rho_+}\middle|\frac{\rho_+}{\rho_-}\right), \tag{2.24}$$

where $\rho_\pm^2$ are the two roots of the polynomial on the right-hand side of (2.23)

$$\rho_\pm^2 = \frac{m_1^2 - a^2 \pm \sqrt{(a^2+m_1^2)^2 - 4m_1^2\pi_2^2}}{2m_1^2}\,. \tag{2.25}$$

The expression for the angle φ_2 is gotten from integrating $\varphi_2' = \pi_2/(1-\rho_1^2)$ and is given by an elliptic integral of the third kind

$$\varphi_2 = \varphi_{2i} \pm \frac{\rho_+\pi_2}{\sqrt{a^2-\pi_2^2}} \Pi\left(\rho_+^2, \arcsin\frac{\rho_1}{\rho_+}\middle|\frac{\rho_+}{\rho_-}\right). \tag{2.26}$$

The kinetic part of the action is

$$\mathcal{S}^{\text{kinetic}}_{S^5} = \frac{T\sqrt{\lambda}}{2\pi}\frac{\sqrt{a^2-\pi_2^2}}{\rho_+}\left[E\left(\arcsin\frac{\rho_1}{\rho_+}\middle|\frac{\rho_+}{\rho_-}\right) - F\left(\arcsin\frac{\rho_1}{\rho_+}\middle|\frac{\rho_+}{\rho_-}\right)\right]. \tag{2.27}$$

There are other expressions that will be better suited for $a^2 < \pi_2^2$.

2.4 More complicated cases

We have studied so far cases with motion only inside an S^3 subspace of S^5, and turned on only one of the rotation parameters m_1, while keeping $m_2 = m_3 = 0$.

To study the more complicated cases it may be useful to turn to the description of the sphere [26, 9] in terms of the elliptic coordinates ζ_1 and ζ_2 that solve the equation $\sum \frac{\rho_i^2}{\zeta - m_i^2} = 0$. Assuming $m_1^2 \leq m_2^2 \leq m_3^2$, then the choice

$$m_1^2 \leq \zeta_1 \leq m_2^2 \leq \zeta_2 \leq m_3^2 \,. \tag{2.28}$$

will cover the range full range $\rho_i \geq 0$. We can go back to our previous coordinates by

$$\begin{aligned} \rho_1 &= \sqrt{\frac{(\zeta_1 - m_1^2)(\zeta_2 - m_1^2)}{(m_1^2 - m_2^2)(m_1^2 - m_2^2)}}\,, \qquad \rho_2 = \sqrt{\frac{(\zeta_1 - m_2^2)(\zeta_2 - m_2^2)}{(m_2^2 - m_1^2)(m_2^2 - m_3^2)}}\,, \\ \rho_3 &= \sqrt{\frac{(\zeta_1 - m_3^2)(\zeta_2 - m_3^2)}{(m_3^2 - m_1^2)(m_3^2 - m_2^2)}}\,. \end{aligned} \tag{2.29}$$

In terms of those coordinates the first integrals are related to hyperelliptic curves, and can be solved in term of the appropriate integrals. Here we will not study the more complicated cases in any detail, as shall become clear in section 4, the above examples are already quite rich. We wish to make only some general comments about those cases.

As noted above, even if the boundary conditions fit within an S^1 equator of S^5, preserving an SO(4) × U(1) subgroup of SO(6), the minimal surface will generically move off the equator into an S^2, breaking the symmetry down to SO(3) × U(1). If we turn on two rotations m_1 and m_2 the boundary conditions will be inside an S^3, but the classical solution will generally extend over an S^4, breaking the symmetry from $\mathrm{U}(1)^3$ to $\mathrm{U}(1)^2 \times \mathbb{Z}_2$.

Such solutions can be written down, but it is not clear that they will be minima of the action. The ansatz assumed rotational symmetry, but if the solution spontaneously breaks some of the symmetry, it may break the rotational symmetry as well.

While we do not expect this to happen in the cases we discussed above, it becomes totally clear that this will have to happen if we turn on all three of the rotation parameters m_i. Consider the expectation value of a single Wilson loop, in order to get a finite action each of the circles with angles φ_i will have to shrink to zero radius, i.e. somewhere along the world-sheet each of the ρ_i will vanish.

The rotationally symmetric ansatz would require this to happen on the same point on the world-sheet, which is impossible since $\sum \rho_i^2 = 1$. So to get a finite action the different ρ_i have to vanish at different positions, and the rotational symmetry will be broken. With two rotations it's possible to have two of the ρ's vanish simultaneously, but it is not clear that this will indeed be a minimum of the action. So some extra caution is required in addressing that case.

3. The AdS_5 ansatz

We will now turn to the AdS_5 part of the σ-model. Again we consider periodic motions for the string, starting with a general ansatz and then specializing to several simpler cases.

The main relation between the AdS_5 and the S^5 parts of the ansatz comes through the Virasoro constraints. Since we already have the S^5 contribution to the world-sheet stress-energy tensor, the Virasoro constraints just read

$$\begin{aligned} T_{\sigma\sigma}^{AdS_5} + \frac{L^2}{8\pi\alpha'} a^2 &= 0\,, \\ T_{\sigma\tau}^{AdS_5} + \frac{L^2}{4\pi\alpha'} \sum_i \pi_i m_i &= 0\,. \end{aligned} \tag{3.1}$$

As in the case of the sphere, a simple description of the system is by taking euclidean AdS_5 as a hypersurface in flat six-dimensional Minkowski space. It is given by the hyperboloid

$$-Y_0^2 + Y_1^2 + Y_2^2 + Y_3^2 + Y_4^2 + Y_5^2 = -L^2\,. \tag{3.2}$$

Now let us define the coordinates r_0, r_1, r_2, v, ϕ_1 and ϕ_2 by

$$\begin{aligned} Y_0 &= L r_0 \cosh v\,, & Y_5 &= L r_0 \sinh v\,, \\ Y_1 &= L r_1 \cos\phi_1\,, & Y_2 &= L r_1 \sin\phi_1\,, \\ Y_3 &= L r_2 \cos\phi_2\,, & Y_4 &= L r_2 \sin\phi_2\,. \end{aligned} \tag{3.3}$$

Those coordinates satisfy the constraint $-r_0^2+r_1^2+r_2^2=-1$, and the metric of the embedding flat Minkowski space is

$$ds^2 = L^2\left(-dr_0^2 + r_0^2 dv^2 + dr_1^2 + r_1^2 d\phi_1^2 + dr_2^2 + r_2^2 d\phi_2^2\right). \tag{3.4}$$

In some of the specific examples we study below we will employ Poincaré coordinates. We replace r_0, r_1, r_2 and v with $\hat{y}$, $\hat{r}_1$ and $\hat{r}_2$ by the relations

$$r_0 = \frac{\sqrt{\hat{y}^2+\hat{r}_1^2+\hat{r}_2^2}}{\hat{y}}\,, \qquad r_1 = \frac{\hat{r}_1}{\hat{y}}\,, \qquad r_2 = \frac{\hat{r}_2}{\hat{y}}\,, \qquad v = \ln\sqrt{\hat{y}^2+\hat{r}_1^2+\hat{r}_2^2}\,. \tag{3.5}$$

In the new coordinates the metric reads

$$ds^2 = \frac{L^2}{\hat{y}^2}\left(d\hat{y}^2 + d\hat{r}_1^2 + \hat{r}_1^2 d\phi_1^2 + d\hat{r}_2^2 + \hat{r}_2^2 d\phi_2^2\right). \tag{3.6}$$

Going back to the embedding coordinates, we consider the following ansatz, which is consistent with the equations of motion

$$r_i = r_i(\sigma)\,, \qquad v = v(\sigma)\,, \qquad \phi_1 = k_1\tau + \alpha_1(\sigma)\,, \qquad \phi_2 = k_2\tau + \alpha_2(\sigma)\,, \tag{3.7}$$

where k_1 and k_2 are arbitrary integers (in this case, when the world-sheet is compact, also the parameters m_i of the S^5 ansatz have to be integers). One could consider also some τ dependence for v, but we will not include that. The action now is

$$\begin{aligned} \mathcal{S}_{AdS_5} = \frac{L^2}{4\pi\alpha'}\int d\sigma\, d\tau [&-r_0'^2 + r_1'^2 + r_2'^2 + r_0^2 v'^2 + r_1^2\alpha_1'^2 + r_2^2\alpha_2'^2 + r_1^2 k_1^2 + r_2^2 k_2^2 + \\ &+ \Lambda\left(-r_0^2 + r_1^2 + r_2^2 + 1\right)]\,. \end{aligned} \tag{3.8}$$

v, α_1 and α_2 are cyclic, so we can express them in terms of the conserved momenta

$$v' = \frac{p_0}{r_0^2}\,, \qquad \alpha_1' = \frac{p_1}{r_1^2}\,, \qquad \alpha_2' = \frac{p_2}{r_2^2}\,. \tag{3.9}$$

The equations of motion for r_0, r_1 and r_2 are

$$\begin{aligned} r_0'' &= \Lambda r_0 - \frac{p_0^2}{r_0^3}\,, \\ r_1'' &= (k_1^2+\Lambda) r_1 + \frac{p_1^2}{r_1^3}\,, \\ r_2'' &= (k_2^2+\Lambda) r_2 + \frac{p_2^2}{r_2^3}\,, \end{aligned} \tag{3.10}$$

It is simple to find the first integral of motion, it's the diagonal component of the AdS_5 contribution to the stress-energy tensor, which one can get by multiplying each of the above equations by the appropriate r_i', summing them and using that $(-r_0^2+r_1^2+r_2^2)'=0$. The result is

$$-r_0'^2 + r_1'^2 + r_2'^2 + \frac{p_0^2}{r_0^2} + \frac{p_1^2}{r_1^2} + \frac{p_2^2}{r_2^2} - r_1^2 k_1^2 - r_2^2 k_2^2 + a^2 = 0\,. \tag{3.11}$$

The integration constant a^2 has to be the same as on the S^5 part of the action, so together the Virasoro constraint is satisfied. Using this we can again replace the potential terms by the kinetic ones to find for the classical action

$$\mathcal{S}_{AdS_5} = \frac{\sqrt{\lambda}}{4\pi}\int d\sigma\, d\tau \left[2(r_1^2 k_1^2 + r_2^2 k_2^2) - a^2\right] = 2S_{AdS_5}^{\text{kinetic}} - \frac{\sqrt{\lambda}}{4\pi} a^2 \delta\sigma T\,. \tag{3.12}$$

When combining this with the contribution of the sphere (2.10) the a^2 terms will cancel each other, leaving us with twice the sum of the kinetic actions. This action will be divergent, due to a missing boundary term [13]. After removing the divergence one finds a finite action that is negative (or zero). This is in contrast to the S^5 case, where the action was positive.

The other integrals of motion are

$$\begin{aligned} I_0 &= r_0^2 - \sum_{i=1}^{2} \frac{1}{k_i^2}\left((r_0 r_i' - r_i r_0')^2 + \frac{p_i^2}{r_i^2} r_0^2 - \frac{p_0^2}{r_0^2} r_i^2\right), \\ I_1 &= r_1^2 - \frac{1}{k_1^2}\left((r_0 r_1' - r_1 r_0')^2 + \frac{p_1^2}{r_1^2} r_0^2 - \frac{p_0^2}{r_0^2} r_1^2\right) + \\ &\quad + \frac{1}{k_1^2 - k_2^2}\left((r_1 r_2' - r_2 r_1')^2 + \frac{p_2^2}{r_2^2} r_1^2 + \frac{p_1^2}{r_1^2} r_2^2\right). \end{aligned} \tag{3.13}$$

We can define I_2 in a similar fashion, but it is not an independent integral, $-I_0 + I_1 + I_2 = -1$. They are also related to the diagonal component of the stress-energy tensor by

$$k_1^2 I_1 + k_2^2 I_2 - p_0^2 + p_1^2 + p_2^2 = a^2\,. \tag{3.14}$$

For completeness let us write the off-diagonal component of the stress-energy tensor

$$T_{\sigma\tau} = \frac{L^2}{4\pi\alpha'}\left(k_1 p_1 + k_2 p_2\right), \tag{3.15}$$

which is also a constant.

So like in the case of the sphere, this periodic ansatz reduces the σ-model to an integrable system similar to the Neumann-Rosochatius system. For any value of the integration constants one can find the appropriate solution, though describing it may be complicated. As before, it is possible to introduce the elliptical coordinates and write the solutions in terms of hyperelliptic integrals.

We will not study the general solution, but instead focus below on some simple cases of planar concentric circles and parallel lines.

3.1 AdS_3 ansatz: circles

The first example we look at is that of a surface that ends along two concentric circles at the boundary of AdS_5. In our coordinate system the boundary of AdS_5, which is a four-sphere, is given by $r_0 \to \infty$. If we switch to the Poincaré patch the boundary will be flat $\mathbb{R}^4$. In the latter case (3.6) we describe a circle on the boundary by a constant $\hat{r}_1$ and $\hat{r}_2 = 0$. In the former we take $r_2 = 0$ and the radius of the circle will be given by the value of v.

So to study concentric circles we will use our general ansatz with $r_2 = \phi_2 = 0$. We can then eliminate r_0 from the equations by the identity $r_0^2 = 1 + r_1^2$ and the Virasoro constraint turns into an equation for r_1

$$r_1'^2 = -a^2 - p_0^2 - p_1^2 + (k_1^2 - a^2)r_1^2 + k_1^2 r_1^4 - \frac{p_1^2}{r_1^2}\,. \tag{3.16}$$

It turns out to be useful to write the equation in terms of $z = 1/r_1$, which goes to zero at the boundary. The above equation becomes

$$z'^2 = k^2 + (k^2 - a^2)z^2 - (a^2 + p_0^2 + p_1^2)z^4 - p_1^2 z^6\,. \tag{3.17}$$

This can be solved in terms of elliptic integrals. In what follows we concentrate on $p_1 = 0$ and label $p_0 = p$. Generically the surfaces will reach the boundary twice, and will correspond to the correlator of two Wilson loops.

For $a^2 + p^2 > 0$ the equation has a turning point, a maximal value of z before the surface goes back to the boundary. For $a^2 + p^2 < 0$ (note that a^2 could be negative) we will have to analytically continue beyond $z = \infty$ to get the second part of the string. The case of $a^2 + p^2 = 0$ is very interesting, and as we will see it generally describes the correlator of the Wilson loop with a local operator. A special case we will concentrate on later is for $p = 0$, where v is constant along the world-sheet. This will describe the correlator of two coincident loops, or in the case of $a^2 = 0$, the one-point function of a Wilson loop. We illustrate some of those solutions in figure 1.

We start with the case of $a^2 + p^2 > 0$, where the solution can be written in terms of elliptic integrals with modulus z_+/z_- and argument $\arcsin z/z_+$ where $z_\pm^2$ are the two roots of the polynomial on the right-hand side of (3.17)

$$z_\pm^2 = \frac{k^2 - a^2 \pm \sqrt{(a^2 + k^2)^2 + 4k^2 p^2}}{2(a^2 + p^2)}\,, \tag{3.18}$$

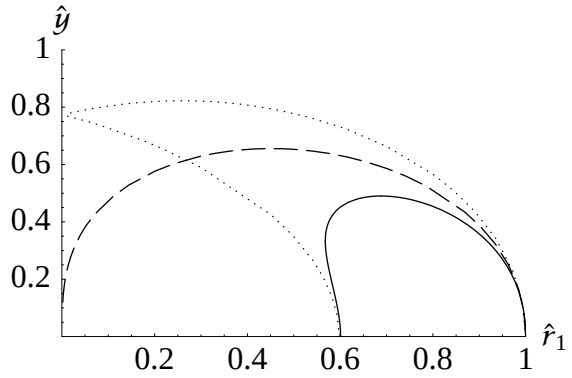

Figure 1: The value of $\hat{y}$ as a function of $\hat{r}_1$ for three solutions to the AdS_3 ansatz. For two circles with radii $R_i = 0.6$ and $R_f = 1$ and opposite orientation (solid line), the solution has $a^2 + p^2 > 0$. If the circles have the same orientation, the surface has to cross $\hat{r}_1 = 0$ which is given by the expressions with $a^2 + p^2 < 0$ (dotted line). For $a^2 + p^2 = 0$ (dashed line) the surface describes the correlator of a circle and a local operator at $\hat{r}_1 = 0$.

as

$$\sigma = \frac{z_+}{k} F\left(\arcsin\frac{z}{z_+}\middle|\frac{z_+}{z_-}\right). \tag{3.19}$$

Inverting this equation gives z, or r_0 and r_1 as a function of σ.

Clearly z has a turning point, or a maximum, at z_+. Beyond there we have to continue on the other branch of the inverse sine function, until reaching the boundary again. That will give the full range of the world-sheet coordinate σ by the complete elliptic integrals

$$\delta\sigma = \frac{2z_+}{k} K\left(\frac{z_+}{z_-}\right). \tag{3.20}$$

Next we can integrate v in terms of elliptic integrals of the first and third kind (v_i is the initial value, at $z = 0$)

$$\begin{aligned} v - v_i &= p\int \frac{d\sigma}{r_0^2} = p\int \frac{dz}{z'}\frac{z^2}{1+z^2} \\ &= \frac{pz_+}{k}\left[F\left(\arcsin\frac{z}{z_+}\middle|\frac{z_+}{z_-}\right) - \Pi\left(-z_+^2, \arcsin\frac{z}{z_+}\middle|\frac{z_+}{z_-}\right)\right]. \end{aligned} \tag{3.21}$$

This expression again covers only half the world-sheet, the other branch is given by a similar expression shifted by the complete elliptic integrals

$$\begin{aligned} v - v_i = \frac{pz_+}{k}\Bigg[&2K\left(\frac{z_+}{z_-}\right) - 2\Pi\left(-z_+^2\middle|\frac{z_+}{z_-}\right) - \\ &- F\left(\arcsin\frac{z}{z_+}\middle|\frac{z_+}{z_-}\right) + \Pi\left(-z_+^2, \arcsin\frac{z}{z_+}\middle|\frac{z_+}{z_-}\right)\Bigg]. \end{aligned} \tag{3.22}$$

The surface started on the first branch at $v = v_i$. On the second branch v reaches the final value v_f, so the total change is

$$\delta v = v_f - v_i = \frac{2pz_+}{k}\left[K\left(\frac{z_+}{z_-}\right) - \Pi\left(-z_+^2\middle|\frac{z_+}{z_-}\right)\right]. \tag{3.23}$$

Recall that in the Poincaré patch (3.6) the boundary of AdS_5 is at $z = 0$, and there the radius $\hat{r}_1 = \exp v$. When considering the correlator of two concentric circles the ratio of their radii is then given by $\exp \delta v$. We will use this when studying specific examples below.

Finally we can evaluate the action. To perform the integral we have to take care to include the two branches, and regularize the divergence near the boundary by the cutoff z_0

$$\begin{aligned} 2\mathcal{S}^{\text{kinetic}}_{AdS_5} &= \frac{\sqrt{\lambda}}{4\pi}\int d\tau\, d\sigma\, 2k^2 r_1^2 = \frac{T\sqrt{\lambda}}{2\pi}\, k^2 \int \frac{dz}{z^2 z'} \\ &= -\frac{T\sqrt{\lambda}}{2\pi}\, 2k\Bigg[\frac{1}{z}\sqrt{(1-\frac{z^2}{z_+^2})\left(1-\frac{z}{z_-^2}\right)} - \\ &\qquad - \frac{1}{z_+}F\left(\arcsin\frac{z}{z_+}\middle|\frac{z_+}{z_-}\right) + \frac{1}{z_+}E\left(\arcsin\frac{z}{z_+}\middle|\frac{z_+}{z_-}\right)\Bigg]_{z_0}^{z_+} \qquad (3.24) \\ &= \frac{T\sqrt{\lambda}}{2\pi}\, 2k\left[\frac{1}{z_0} - \frac{1}{z_+}E\left(\frac{z_+}{z_-}\right) + \frac{1}{z_+}K\left(\frac{z_+}{z_-}\right)\right]. \qquad (3.25) \end{aligned}$$

The divergent term is proportional to the circumference of the circle, and is canceled by a boundary term. Thus the kinetic part of the action will be given just by the complete elliptic integrals. Note that in this case of the circles the range of the τ variable is $T = 2\pi$, but we have chosen to leave the explicit dependence on T in the expressions.

Next, we will consider the $a^2 + p^2 = 0$ case (also studied in [18]), and argue that it describes a two-point function of a Wilson loop and a local operator. We define $b^2 = -a^2$, so we have $b = \pm p$ and the solution for z is simply

$$z = \frac{k}{\sqrt{k^2+p^2}}\sinh\left(\sqrt{k^2+p^2}\,\sigma\right), \qquad (3.26)$$

and for v we get

$$v = p\sigma - \operatorname{arctanh}\left(\frac{p}{\sqrt{k^2+p^2}}\tanh\sqrt{k^2+p^2}\,\sigma\right). \qquad (3.27)$$

Both expressions diverge as $\sigma \to \infty$. To understand the geometry it's useful to switch to the Poincaré patch (3.6) where

$$\hat{r}_1 = \frac{e^v}{\sqrt{1+z^2}}, \qquad \hat{y} = \frac{z e^v}{\sqrt{1+z^2}}. \qquad (3.28)$$

If we choose the solution with negative p, we find that $v \to -\infty$, so the surface gets back to the boundary at $\hat{r}_1 = 0$, so instead of calculating the correlator of two Wilson loops, this describes the two-point function of a Wilson loop and a local operator at $\hat{r}_1 = 0$. The case with positive p, or $v \to \infty$ gives a similar surface, for a local operator inserted at infinite $\hat{r}_1$.

The action in this case is

$$2\mathcal{S}^{\text{kinetic}}_{AdS_5} = -\frac{T\sqrt{\lambda}}{2\pi}\sqrt{k^2+p^2}\,\coth\sqrt{k^2+p^2}\,\sigma\Big|_{\sigma_{\min}}^{\sigma_{\max}}. \qquad (3.29)$$

$\sigma_{\min}$ and $\sigma_{\max}$ are chosen such that $\hat{y} = \hat{y}_0$, some cutoff. Near $\sigma = 0$ there is the usual linear divergence which will cancel against a boundary term giving

$$2\mathcal{S}^{\text{kinetic}}_{AdS_5} = -\frac{T\sqrt{\lambda}}{2\pi}\sqrt{k^2+p^2}\,. \tag{3.30}$$

There is another potential divergence at $\sigma \to \infty$. The full AdS_5 action (3.12) includes a term proportional to the area of the world-sheet, which will diverge logarithmically with $\hat{y}_0$. In all the cases we study this term will cancel against an equal contribution from the σ-model on the sphere. But it is possible that there are cases when those terms will not cancel exactly, then this logarithmic divergence will capture the anomalous dimension of the local operator.

For $a^2 + p^2 < 0$, equation (3.17) again doesn't have a turning point, so the surface reaches $z = \infty$. Beyond that point we should continue the solution to another branch, until it comes back to the boundary. It again describes the correlator of two circles, but since the surface crosses itself at infinite z (or $r_1 = 0$), the orientation of the circles will be the opposite of the previous examples. Now the two circles are oriented in the same direction, so the surface that connects them has to cross itself to preserve this orientation.

In this case both z_+ and z_- defined in (3.18) are imaginary, therefore it is useful to define $b^2 = -a^2$ and use

$$\tilde{z}^2_\pm = \frac{b^2+k^2 \pm \sqrt{(b^2-k^2)^2+4k^2p^2}}{2(b^2-p^2)} = -z^2_\pm\,. \tag{3.31}$$

Then the solution is conveniently written in terms of elliptic integrals with the complementary modulus $\sqrt{1-\tilde{z}^2_+/\tilde{z}^2_-}$ as

$$\sigma = \frac{\tilde{z}_+}{k} F\left(\arctan\frac{z}{\tilde{z}_+}\middle|\sqrt{1-\frac{\tilde{z}^2_+}{\tilde{z}^2_-}}\right). \tag{3.32}$$

Indeed we see that z can extend to infinity, which corresponds to $r_1 = 0$, beyond which we have to analytically continue σ. The solution will reach the boundary $z = 0$ again at $\arctan z/\tilde{z}_+ = \pi$, so the full range of σ is twice the complete elliptic integral

$$\delta\sigma = \frac{2\tilde{z}_+}{k} K\left(\sqrt{1-\frac{\tilde{z}^2_+}{\tilde{z}^2_-}}\right). \tag{3.33}$$

Next we integrate v

$$\begin{aligned} v - v_i = \frac{p\tilde{z}^3_+}{k(\tilde{z}^2_+-1)}\Bigg[&F\left(\arctan\frac{z}{\tilde{z}_+}\middle|\sqrt{1-\frac{\tilde{z}^2_+}{\tilde{z}^2_-}}\right) - \\ &- \Pi\left(1-\tilde{z}^2_+,\arctan\frac{z}{\tilde{z}_+}\middle|\sqrt{1-\frac{\tilde{z}^2_+}{\tilde{z}^2_-}}\right)\Bigg]. \end{aligned} \tag{3.34}$$

As before, this covers half the world-sheet, and the other branch is found in the same manner. On the second branch v reaches the final value

$$\delta v = v_f - v_i = \frac{2p\tilde{z}^3_+}{k(\tilde{z}^2_+-1)}\left[K\left(\sqrt{1-\frac{\tilde{z}^2_+}{\tilde{z}^2_-}}\right) - \Pi\left(1-\tilde{z}^2_+\middle|\sqrt{1-\frac{\tilde{z}^2_+}{\tilde{z}^2_-}}\right)\right]. \tag{3.35}$$

Finally we evaluate the action, which after removing the standard divergence is

$$2\mathcal{S}^{\text{kinetic}}_{AdS_5} = -\frac{T\sqrt{\lambda}}{2\pi}\,\frac{2k}{\tilde{z}_+}\,E\left(\sqrt{1-\frac{\tilde{z}_+^2}{\tilde{z}_-^2}}\right). \tag{3.36}$$

3.2 AdS_2 ansatz: circles

Let us now consider the simpler case where v is a constant, or $p = 0$. At the boundary of AdS_5 the value of v is related to the radius of the circle by $R = \exp v$ (3.5), so this corresponds to a single circle or two coincident circles on the boundary. This ansatz involves only the coordinates z and ϕ_1 (or r_0, r_1 and ϕ_1), which parameterize an AdS_2 subspace of AdS_5, hence the name.

In the Poincaré coordinates (3.6) both $\hat{y}$ and $\hat{r}_1$ will be non-zero, but they will satisfy the constraint

$$\hat{y}^2 + \hat{r}_1^2 = R^2\,, \tag{3.37}$$

with R clearly the radius of the circle on the boundary.

For $a^2 > 0$, the solution is the same as the more general case (3.19), with the replacement (3.18) of $z_+ = a/k$ and $z_- = i$

$$\sigma = \frac{1}{a}F\left(\arcsin\frac{az}{k}\middle|\, i\frac{k}{a}\right). \tag{3.38}$$

The coordinate z takes values between 0, the boundary of AdS_5 and $z_+ = k/a$, where it folds back on itself, reaching again the boundary of AdS_5. The solution therefore covers twice a region of a Poincaré disk, delimited by the boundary and a finite radius. Between the two points where the surface reaches the boundary, the world-sheet coordinate $a\sigma$ will extend from 0 to twice the complete elliptic integral. Thus the range of the world-sheet coordinate σ is given by

$$\delta\sigma = \frac{2}{a}K\left(i\frac{k}{a}\right). \tag{3.39}$$

We can evaluate the action, where after accounting for the two branches, and removing the divergence we find

$$2\mathcal{S}^{\text{kinetic}}_{AdS_5} = -\frac{T\sqrt{\lambda}}{2\pi}\,2a\left[E\left(i\frac{k}{a}\right) - K\left(i\frac{k}{a}\right)\right]. \tag{3.40}$$

If $a = 0$ the solution is even simpler

$$z = \sinh k\sigma\,. \tag{3.41}$$

In the Poincaré coordinates (3.6) this translates to

$$\hat{y} = R\tanh k\sigma\,, \qquad \hat{r}_1 = \frac{R}{\cosh k\sigma}\,, \tag{3.42}$$

where $R = \exp v$ is the radius of the circle on the boundary. The action in this case is (after subtracting the divergence)

$$\mathcal{S}_{AdS_5} = -\frac{T\sqrt{\lambda}}{2\pi}\,k\,. \tag{3.43}$$

This solution is different from the case $a^2 + p^2 = 0$ considered above. Here the surface does not reach the boundary again as $z \to \infty$, instead we reach $\hat{y} = R$, where the surface can connect to itself. Thus this surface will describe a single Wilson loop. Since $T = 2\pi$, the action is simply k times the result for the simplest circular observable [12, 13].

For $a^2 < 0$, the z coordinate again extends to infinity, or r_1 reaches zero. But now the surface will not close smoothly on itself. Instead we have to continue it beyond that point, until it reaches the boundary again. Defining $b^2 = -a^2$ we have the general case with the replacement $\tilde{z}_+ = 1$ and $\tilde{z}_- = k/b$

$$\sigma = \frac{1}{k} F\left(\arctan z \middle| \sqrt{1 - \frac{b^2}{k^2}}\right). \tag{3.44}$$

The range of σ is again twice the complete elliptic integral, which we write in two ways utilizing the symmetry of exchanging the two roots $\tilde{z}_+ \leftrightarrow \tilde{z}_-$

$$\delta\sigma = \frac{2}{k} K\left(\sqrt{1 - \frac{b^2}{k^2}}\right) = \frac{2}{b} K\left(\sqrt{1 - \frac{k^2}{b^2}}\right), \tag{3.45}$$

and the action is

$$2\mathcal{S}^{\text{kinetic}}_{AdS_5} = -\frac{T\sqrt{\lambda}}{2\pi}\, 2k\, E\left(\sqrt{1 - \frac{b^2}{k^2}}\right). \tag{3.46}$$

3.3 AdS_3 ansatz: straight lines

We now wish to consider the case of infinite anti-parallel straight lines. This is a degenerate example of the planar circles, which corresponds to taking the double limit of nearly coincident circles of very large radii. Yet, since the anti-parallel lines are very natural observables, which capture the potential between external charged particles, we derive the results in detail.

Consider two lines extended in the x_1 direction separated in the x_2 direction at the boundary of the Poincaré patch. This naturally leads to the ansatz (in what follows we omit the hats to avoid clutter),

$$x_1 = \tau\,, \qquad y = y(\sigma)\,, \qquad x_2 = x_2(\sigma)\,, \tag{3.47}$$

which produces the following AdS_5 action

$$\mathcal{S}_{AdS_5} = \frac{L^2}{4\pi\alpha'} \int d\sigma\, d\tau\, \frac{1 + y'^2 + x_2'^2}{y^2}\,. \tag{3.48}$$

The coordinate x_2 is cyclic, with a conserved momentum $p = x_2'/y^2$.

The equation of motion for y

$$\frac{yy'' - y'^2 + 1}{y^3} + p^2 y = 0\,, \tag{3.49}$$

is integrated once to yield

$$\frac{y'^2 - 1}{y^2} + p^2 y^2 = -a^2\,. \tag{3.50}$$

Note that as before, the left hand side is proportional to the AdS_5 contribution to the diagonal part of the stress-energy tensor, therefore the constant on the right hand side has to be equal to the integration constant on the sphere. And again we express the on-shell action in terms of the kinetic term

$$\mathcal{S}_{AdS_5} = \frac{\sqrt{\lambda}}{4\pi}\int d\sigma\, d\tau\, \left(\frac{2}{y^2} - a^2\right) = 2S^{\text{kinetic}}_{AdS_5} - \frac{\sqrt{\lambda}}{4\pi}\int d\sigma\, d\tau\, a^2\,. \tag{3.51}$$

Comparing the equation for y (3.50) to the equation for z above (3.17) we see that this is a degenerate case when we replace

$$z \to ky\,, \qquad p \to \frac{p}{k}\,, \tag{3.52}$$

and take the limit of $k \to 0$. So all the formulae below will follow from the previous ones in this limit.

Unless $p^2 = 0$ and $a^2 \leq 0$, y will have a turning point at

$$y_+^2 = \frac{-a^2 + \sqrt{a^4 + 4p^2}}{2p^2}\,. \tag{3.53}$$

The equation can be solved in terms of an elliptic integral of the first kind with modulus $ipy_+^2 = y_+/y_-$, where y_- is the other root of (3.50)

$$\sigma = y_+ F\left(\arcsin\frac{y}{y_+}\middle|\, ipy_+^2\right), \tag{3.54}$$

Varying y between zero and y_+ corresponds to σ/y_+ going from 0 to the complete elliptic integral. Unless we study the single straight line, this range covers only half the world-sheet, so we have to take care to multiply some quantities by two to fix that. Thus

$$\delta\sigma = 2y_+ K\left(ipy_+^2\right). \tag{3.55}$$

x_2 in turn can be written in terms of elliptic integrals of the first and second kind

$$x_2 = p\int d\sigma\, y^2 = \frac{1}{py_+}\left[E\left(\arcsin\frac{y}{y_+}\middle|\, ipy_+^2\right) - F\left(\arcsin\frac{y_+}{y}\middle|\, ipy_+^2\right)\right]. \tag{3.56}$$

The distance between the lines is given by the complete integrals

$$R = \frac{2}{py_+}\left[E\left(ipy_+^2\right) - K\left(ipy_+^2\right)\right]. \tag{3.57}$$

The constant a is determined from the solution of the S^5 equation, leaving this expression for R to fix the integration constant p. Scale invariance of the theory means that there is a simple scaling law, $p^{1/2}R$ depends only on the ratio p/a^2.

We can calculate the action, by the same integrals as in the case of the circle (3.40), accounting for the two halves of the world-sheet and removing the divergence we find

$$2\mathcal{S}^{\text{kinetic}}_{AdS_5} = -\frac{T\sqrt{\lambda}}{2\pi}\,\frac{2}{y_+}\left[E\left(ipy_+^2\right) - K\left(ipy_+^2\right)\right] \tag{3.58}$$

where T is the length of the lines

3.4 AdS_2 ansatz: straight lines

A simple case is when $p = 0$, which means the solution has no dependence on the x_2 direction, or in other words $R = 0$ (or $R \to \infty$). Like in the case of the circles, this is the AdS_2 degeneration of the AdS_3 ansatz. This solution will describe two coincident lines or a single line.

For $a^2 > 0$ the solution is

$$y(\sigma) = \frac{1}{a} \sin a\sigma \,, \tag{3.59}$$

and the surface reaches the boundary twice, at $\sigma = 0$ and at $\sigma = \pi/a$. The kinetic part of the action is

$$\mathcal{S}^{\text{kinetic}}_{AdS_5} = \frac{\sqrt{\lambda}}{2\pi} \int d\sigma \, d\tau \frac{1}{y^2} = \frac{T\sqrt{\lambda}}{2\pi} \frac{2}{y_0} \,. \tag{3.60}$$

So after removing the divergence the action vanishes.

In the special case when $a^2 = 0$ the solution is even simpler, $y(\sigma) = \sigma$, and it describes a single straight line. The action again will vanish.

Finally, for $a^2 < 0$ the solution is better written in terms of $b^2 = -a^2$ as

$$y(\sigma) = \frac{1}{b} \sinh b\sigma \,. \tag{3.61}$$

This solution extends to infinite y, but like in the case of the circle with negative a^2, it carries momentum at infinity, and perhaps should be connected to another solution there describing the correlator of two lines with the same orientation. The range of σ now diverges, but since we have not found corresponding solutions to the S^5 ansatz, we cannot realize this example.

3.5 More complicated cases

We have discussed certain solutions that fit within AdS_2 and AdS_3 subspaces of AdS_5, or Wilson loop operators that fit within a plane (or an S^2) on the boundary. But our general ansatz allows much more general solutions.

First, still within the AdS_3 ansatz it is possible to consider the case where $p_1 \neq 0$. The solution of equation (3.17) is still an elliptic integral. So the expressions will be similar to the once above, only somewhat more involved. The real difference comes because now the off-diagonal Virasoro constraint, which includes $k_1 p_1$, will not be satisfied within AdS_5 alone. To fix that we have to take $m_1 \pi_1$ in the S^5 ansatz non-zero too.

The effect of this is to include some extra phase shift along the world-sheet. If one considers, say, the two circles, one boundary will be given by $\phi_{1i} = k_1 \tau$, and the other by $\phi_{1f} = \alpha_1(\delta\sigma) + k_1\tau$. The relative phase will be non-zero if $p_1 \neq 0$, and will be meaningful only if there is some rotation (say m_1) on S^5. Therefore turning on p_1 corresponds exactly to that case with a relative phase between the lines. We will not study this case in detail.

This generalization is still within the AdS_3 subspace, but our ansatz allows much more general solutions, mainly turning on k_2. That will correspond to a Wilson loop that wraps two circles on orthogonal planes on the boundary. Again we can consider the one-point

function of this operator, or the correlator of two. Another case is when we take the radius of one of the circles to infinity, which will give a helix. A solution corresponding to the correlator of two helices was already presented in [27].

We have not studied those cases in detail, and in particular have not checked whether the periodic ansatz used here will always give the true minimum of the action. As mentioned above, in the S^5 case, there are reasons to believe that the symmetric solution will not always give the minimum of the action, so one should take care in studying these examples.

4. Classification of solutions

After studying those general solutions on the sphere and in AdS_5 we put them together here, pointing out special features that arise in the different examples. A lot of the examples were studied over the past years, we try to collect the known facts about those cases, and discuss some new solutions.

4.1 AdS_2 subspace

We start with a very familiar example, where the Wilson loop couples only to one of the scalars, leading to a trivial S^5 ansatz, and also the spatial part is the simplest, either a single line, or a circle.

The straight line is given by (1.2) and (1.6) with $\theta = \pi/2$ and $m_1 = 0$. The solution for the S^5 part is trivial leading to $a^2 = 0$, and in AdS_5 the solution is simply

$$x_1 = \tau\,, \qquad y = \sigma\,, \tag{4.1}$$

This Wilson loop preserves half of the supersymmetry of the theory, and its expectation value is trivial $\langle W \rangle = 1$. The surface described by the above coordinates has a geometry of AdS_2.

A more interesting example is the circular Wilson loop (1.3), with arbitrary wrapping k. The minimal surface is given by (3.41)

$$\phi_1 = k\tau\,, \qquad z = \sinh k\sigma \tag{4.2}$$

or in the other coordinate system

$$\phi_1 = k\tau\,, \qquad \hat{r}_1 = \frac{R}{\cosh k\sigma}\,, \qquad \hat{y} = R\tanh k\sigma\,. \tag{4.3}$$

This surface again has the geometry of AdS_2, but now the action (3.43) is given by $\mathcal{S} = -k\sqrt{\lambda}$, so the expectation value of the Wilson loop is

$$\langle W \rangle = \exp k\sqrt{\lambda}\,. \tag{4.4}$$

This Wilson loop also preserves half the supersymmetries [28, 27], but all the supercharges it preserves involve the superconformal generators, so they do not close on the hamiltonian, and apparently do not force the expectation value to be trivial.

In fact the straight line and the circle are related by a conformal transformation. The difference between the two was attributed [15] to an anomaly that arises since the conformal transformation takes the point at infinity where the line ends, to a finite distance.

Quite remarkably one can reproduce this result from a perturbative calculation assuming only ladder/rainbow diagrams contribute (in the Feynman gauge) [14]. The exact result at finite N from this gauge theory calculation is captured by the hermitean matrix model given by the following integral over all $N \times N$ hermitean matrices M

$$\langle W_{\text{ladders}} \rangle = \left\langle \frac{1}{N} \operatorname{Tr} \exp M \right\rangle = \frac{1}{Z} \int \mathcal{D}M \frac{1}{N} \operatorname{Tr}(\exp kM) \exp\left(-\frac{2N}{\lambda} \operatorname{Tr} M^2 \right). \tag{4.5}$$

The leading behavior at large N, expressed in terms of the modified Bessel function, is easily found using Wigner's semi-circle law

$$\langle W_{\text{ladders}} \rangle \sim \int_{-1}^{1} dx \sqrt{1-x^2} \exp\left(xk\sqrt{\lambda} \right) = \frac{2}{k\sqrt{\lambda}} I_1\left(k\sqrt{\lambda} \right) \sim \exp k\sqrt{\lambda}\,. \tag{4.6}$$

This is indeed the leading behavior of the circular Wilson loop as calculated by the string in AdS_5.

One can do better and solve this matrix model exactly applying several different techniques. Using orthogonal polynomials, the full result at finite N was given [15, 29] in terms of a Laguerre polynomial $L_n^k(x) = 1/n! \exp[x] x^{-k} (d/dx)^n (\exp[-x] x^{n+k})$ as

$$\langle W_{\text{ladders}} \rangle = \left\langle \frac{1}{N} \operatorname{Tr} \exp M \right\rangle = \frac{1}{N} L_{N-1}^1 \left(-\frac{k^2\lambda}{4N} \right) \exp\left(\frac{k^2\lambda}{8N} \right), \tag{4.7}$$

Several properties of this result, expanded at large N and λ were compared to the expected behavior of semiclassical string in AdS_5.

The most extensive test of this expression was carried out in [16] where all the non-planar corrections at large N and large λ with fixed ration $k^2\lambda/N$ were evaluated. The result

$$\exp\left[-\frac{k\sqrt{\lambda}}{2} \sqrt{1 + \frac{k^2\lambda}{16N^2}} - 2N \operatorname{arcsinh} \frac{k\sqrt{\lambda}}{4N} \right], \tag{4.8}$$

was then compared to a calculation of the Wilson loop using a D3-brane instead of a fundamental string. The results were in complete agreement capturing all quantum corrections beyond the leading planar result.

While this AdS_2 sector includes non-trivial Wilson loops only along the circle, there is an infinite family of Wilson loops one may consider. Here we discussed only the single trace operator of the Wilson loop wrapped k times, but there are multi-trace Wilson loops. Some were calculated in [15], and the resulting expressions are rather complicated. Alternatively, one may consider Wilson loops in higher dimensional representations of the gauge group.

4.2 $AdS_3 \times S^1$ subspace

The AdS_2 example has many interesting features, but in terms of finding the minimal surface solution, it's extremely trivial. So we turn now to the $AdS_3 \times S^1$ subspace. In the previous example the Wilson loop was along a one-dimensional line or circle, and the

resulting surface had the geometry of AdS_2. In general if the Wilson loop is planar, the resulting minimal surface will sit within an AdS_3 subspace of AdS_5, since the solution will depend only on the two coordinates on the plane and the radial coordinate $\hat{y}$.

The same is true for operators that are defined along a curve inside any 2-sphere on the boundary of AdS_5. One can stereographically project any 2-sphere to a plane, and unless a point along the Wilson loop is mapped to infinity, the result of the calculation will not be altered.

The periodic solutions that fit in this sector correspond to two anti-parallel lines (i.e. (1.2) at two values of x_2 separated by R), or two concentric circles (i.e. (1.3) with radii R_i and R_f). In addition we allow the two lines to couple to different scalars, (i.e. (1.6) with $\theta = \pi/2$, $m_1 = 0$ and $\varphi_1 = \varphi_{1i}$ on one line and $\varphi_1 = \varphi_{1f}$ on the second).

The minimal solution will fit within an $S^1 \subset S^5$. That ansatz has $a^2 > 0$ which will select the $a^2 + p^2 > 0$ case of the AdS_3 ansatz.

4.2.1 Anti-parallel lines

Here we study the example of two infinite anti-parallel straight lines, extended in the x_1 direction and located at $x_2 = \pm R/2$. In addition to the separation in space, we allow the lines to be at different points on S^5. So the boundary conditions along the first line are

$$x_1 = \tau\,, \qquad x_2 = -\frac{R}{2}\,, \qquad \varphi_1 = \varphi_{1i}\,, \tag{4.9}$$

and along the second line

$$x_1 = \tau\,, \qquad x_2 = \frac{R}{2}\,, \qquad \varphi_1 = \varphi_{1f}\,. \tag{4.10}$$

This type of Wilson loops was the one studied in the original papers of Rey and Yee and of Maldacena [19, 20]. Already in [20] the two lines were allowed to be at different positions on S^5. As explained in section 2.1, this corresponds to turning on only the integration constant π_1 in (2.6). All the m_i in our general ansatz (2.4) as well as π_2 and π_3 are set to zero and we take $\rho_1 = 1$ and $\rho_2 = \rho_3 = 0$.

So only the angle φ_1 will vary along the world-sheet and is given by $\varphi_1 = \varphi_{1i} + \pi_1\sigma$. The constant a in the Virasoro constraint is given by $a = \pi_1$ and the range of the world-sheet coordinate σ is

$$\delta\sigma = \frac{\delta\varphi_1}{a}\,, \tag{4.11}$$

where the two lines are separated by an angle $\delta\varphi_1$.

In the general ansatz for parallel lines (section 3.3) we use the same constant a and the range of σ was given by the complete elliptic integral (3.55)

$$\delta\sigma = 2y_+ K\left(ipy_+^2\right) \tag{4.12}$$

with (3.53)

$$y_+^2 = \frac{-a^2 + \sqrt{a^4 + 4p^2}}{2p^2}\,. \tag{4.13}$$

Equating those two expressions for $\delta\sigma$ gives a relation between $\delta\varphi_1$ and p/a^2. This simple scaling is a consequence of conformal invariance, the distance between two parallel lines can be changed by a conformal transformation. Equation (3.57)

$$R = \frac{2}{y_+ p}\left[E\left(ipy_+^2\right) - K\left(ipy_+^2\right)\right], \tag{4.14}$$

gives $R\sqrt{p}$ as a function of p/a^2, and then by the previous relation in terms of $\delta\varphi_1$.

The full action for this solution is given by twice the sum of the kinetic terms on S^5, which vanishes in this case, and the AdS_5 part (3.58). The result is

$$\mathcal{S} = -\frac{T\sqrt{\lambda}}{2\pi}\frac{2}{y_+}\left[E\left(ipy_+^2\right) - K\left(ipy_+^2\right)\right] = -\frac{T\sqrt{\lambda}}{2\pi}pR\,. \tag{4.15}$$

This is a simple way of writing the action, but the right-hand-side is not expressed solely in terms of the geometric data, R and $\delta\varphi_1$. To fix that one uses the above relations to replace for p, which will be $1/R^2$ times some function of $\delta\varphi_1$. Then the right-hand side will always exhibit a Coulomb-like potential.

If the two lines are at the same value of φ_1, the solution simplifies. We set $a = 0$, and find [19, 20]

$$R = \frac{2}{\sqrt{p}}\left[E(i) - K(i)\right] = \frac{(2\pi)^{3/2}}{\Gamma(1/4)^2\sqrt{p}}\,. \tag{4.16}$$

Using (3.58) we evaluate the action, which after subtracting the divergence is

$$\mathcal{S} = -\frac{\sqrt{\lambda}}{2\pi}(R\sqrt{p})^2\frac{T}{R} = -\frac{4\pi^2\sqrt{\lambda}}{\Gamma(1/4)^4}\frac{T}{R}\,. \tag{4.17}$$

It is worth pointing out that even in this simple case, the boundary conditions allow for another solution: two disconnected surfaces as in equation (4.1) corresponding each to a single straight line. The action for this solution is zero, and the action for the connected solution (4.15) is always negative, so in this case the connected solution dominates for any value of the geometric data, R and $\delta\varphi_1$. In more general cases, different solutions will dominate in different ranges of the parameters, as we will see in the next example.

4.2.2 Concentric circles

A richer example is that of two concentric circles in a plane in $\mathbb{R}^4$. The new feature that arises is that for certain values of the radii, the connected classical solution ceases to exist. This phenomenon was described in this context first by Gross and Ooguri [30]. They used the intuition from flat space where two circles on parallel planes have a connected minimal surface between them only if they are separated by a distance smaller than roughly 1.325 times their radius.

This configuration was studied in AdS_5 space in [21, 22], where two concentric circles of equal or unequal radii on two parallel planes where considered. In our ansatz we study circles in the same plane, but those solutions are not really different. Two concentric circles on parallel planes define a 2-sphere or a plane in $\mathbb{R}^4$. Since we can relate any 2-sphere to

JHEP01(2006)056

the plane by a conformal transformation, those systems are equivalent. We repeat the calculation here, generalizing it by allowing the two circles to have different values for the S^5 angle φ_1.

Now the boundary conditions on the string along the first circle are

$$\phi_1 = k\tau\,, \qquad v = v_i\,, \qquad \varphi_1 = \varphi_{1i}\,, \tag{4.18}$$

and along the second circle

$$\phi_1 = k\tau\,, \qquad v = v_f\,, \qquad \varphi_1 = \varphi_{1f}\,. \tag{4.19}$$

By conformal invariance, the result ought to depend only on the ratio of the radii, which according to (3.5) is given by $R_f/R_i = \exp(v_f - v_i)$.

As in the case of the parallel lines, we have to relate the range of the world-sheet coordinate σ in the two parts of the ansatz. From (2.11) and (3.20) we get the relation

$$\delta\sigma = \frac{\delta\varphi_1}{a} = \frac{2z_+}{k} K\left(\frac{z_+}{z_-}\right), \tag{4.20}$$

with (3.18)

$$z_\pm^2 = \frac{k^2 - a^2 \pm \sqrt{(a^2+k^2)^2 + 4k^2p^2}}{2(a^2+p^2)}\,, \tag{4.21}$$

A second equation comes from the boundary conditions on v. The total shift in v is given by (3.23)

$$\delta v = v_f - v_i = \log\frac{R_f}{R_i} = \frac{2pz_+}{k}\left[K\left(\frac{z_+}{z_-}\right) - \Pi\left(-z_+^2\,\middle|\,\frac{z_+}{z_-}\right)\right]. \tag{4.22}$$

The full action is again twice the sum of the kinetic terms, which vanishes for this S^1 ansatz, so it's just the AdS_5 contribution restricted to the AdS_3 case (3.25), with $T = 2\pi$

$$\mathcal{S} = -\sqrt{\lambda}\,\frac{2k}{z_+}\left[E\left(\frac{z_+}{z_-}\right) - K\left(\frac{z_+}{z_-}\right)\right]. \tag{4.23}$$

One can always construct also a disconnected solution, each of the circles will be the boundary of the world-sheet described in section 4.1. The action for the disconnected solution doesn't depend on the ratio of radii, it's simply twice the action there, $\mathcal{S} = -2k\sqrt{\lambda}$. The Gross-Ooguri phase transition [30] will take place when the action of the connected solution reaches this value. In the case with $\delta\varphi_1 = 0$ this happens at $R_f/R_i \sim 2.4034$.

Furthermore, for any fixed value of $\delta\varphi_1$, by plotting δv, one can see that it reaches a maximum, which implies that we have connected surfaces only for a finite range of the ratio of radii. Beyond that, only the disconnected solution exists. For $\delta\varphi_1 = 0$, this happens for $K(z_+/z_-) = 2E(z_+/z_-)/(1 - z_+^2/z_-^2)$ or roughly $p/k \sim 0.5811$. This value corresponds to a ratio $R_f/R_i \sim 2.7245$, and was already obtained by Zarembo and Olesen [21, 22], who considered the correlator of two circles in parallel planes separated by a distance L. Their configuration and ours are conformally related by a stereographic projection.

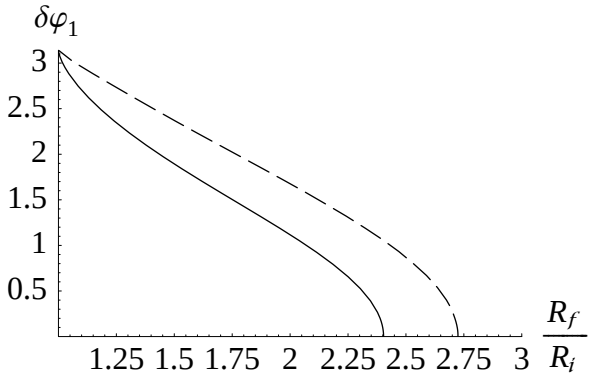

Figure 2: The allowed range of R_f/R_i for two circles of radii $R_f \geq R_i$ as a function of the separation on the sphere, $\delta\varphi_1$. Connected classical solutions exist for all values inside the region bound by the dashed line. This connected solution dominates only inside the region bound by the solid line.

We illustrate this in figure 2. A connected solution exists only inside the dashed curve. Inside the solid curve this connected solution has lower action than the disconnected one and will dominate. The closer the initial and final values of R are, the range of $\delta\varphi_1$ with a connected solution will increase. This graph is symmetric under the inversion $R_f/R_i \to R_i/R_f$.

4.3 $AdS_2 \times S^2$ subspace

We consider now the case where on the boundary of AdS_5 the source is localized along a line or a circle and on the S^5 part the ansatz will involve periodic motion inside a 2-sphere. This ansatz includes single lines, or circles with some rotation on S^2, and may also include the correlator of two lines/circles, as long as they are separated only in the S^5 directions. This sector obviously includes the line and circle with no rotation reviewed in section 4.1. Another case already studied in section 4.2 is that of two coincident lines or circles separated on the sphere by a constant angle $\delta\varphi_1$.

4.3.1 Single line

We first review the case of a single straight line, already presented in [24]. The Wilson loop will be the line (1.2) with periodic coupling to three of the scalars, (1.6) with $\cos\psi = 0$ and only $m_1 = m$ non-zero. The minimal surface will be given by the S^2 solution discussed in section 2.2 in the special case of $a = 0$, and the simplest AdS_2 ansatz. The solution is

$$x_1 = \tau\,, \qquad y = \sigma\,, \qquad \varphi_1 = m\tau\,, \qquad \sin\theta = \frac{1}{\cosh m(\pm\sigma + \sigma_i)}\,. \tag{4.24}$$

The world-sheet extends from $\sigma = 0$ to infinity and σ_i is set by the boundary value of θ as $\sin\theta_i = 1/\cosh m\sigma_i$. The choice of sign corresponds to the surface covering the northern or southern hemisphere, one of which will be a minimum and the other an unstable saddle point (unless $\theta_i = \pi/2$).

The AdS_5 part of the solution is identical to the usual straight line (4.1), whose action vanishes (after including the boundary term). The action therefore comes from the S^5 part, and is equal to the area of the part of the sphere covered by the surface a certain number of times (2.14)

$$\mathcal{S} = \frac{\sqrt{\lambda}}{2\pi} T m \left(1 - |\cos\theta_i|\right), \tag{4.25}$$

where T is a regulator of the length of the line.

4.3.2 Single circle

Next we consider the expectation value of a Wilson loop which is wrapped k times around a circle (1.6) while wrapping m times a parallel at angle θ_i on S^2.

Again the constant a vanishes so the solution of the sphere σ-model is like in the above example, while for the AdS_5 part we use (3.41) giving

$$\phi_1 = k\tau\,, \qquad z = \sinh k\sigma\,, \qquad \varphi_1 = m\tau\,, \qquad \sin\theta = \frac{1}{\cosh m(\pm\sigma + \sigma_i)}\,, \tag{4.26}$$

Again the sign corresponds to a surface extending over the northern or southern hemisphere and is chosen to minimize the action, and at $\sigma = 0$ the boundary value of $\sin\theta$ is set to $1/\cosh m\sigma_i$. We also write the solution in terms of the coordinates on the Poincaré patch

$$\hat{y} = R\tanh k\sigma\,, \qquad \hat{r}_1 = \frac{R}{\cosh k\sigma}\,. \tag{4.27}$$

Note that $\hat{y}^2 + \hat{r}_1^2 = R^2$.

The contribution to the action from the AdS_5 part (3.43) is k times that of the regular circle, or $\mathcal{S}_{AdS_5} = -k\sqrt{\lambda}$. From the S^5 part we get the area of the part of the sphere covered by the surface $\mathcal{S}_{S^5} = m\sqrt{\lambda}(1 - |\cos\theta_i|)$. Together the action is

$$\mathcal{S} = \left(-k + m - m|\cos\theta_i|\right)\sqrt{\lambda}\,. \tag{4.28}$$

Thus the expectation value of the Wilson loop at strong coupling is given by

$$\langle W\rangle \sim \exp\left[(k - m + m|\cos\theta_i|)\sqrt{\lambda}\right]. \tag{4.29}$$

Note here that in the special case when $m = k$ this reduces to

$$\langle W\rangle \sim \exp\left[k\cos\theta_i\sqrt{\lambda}\right], \tag{4.30}$$

which will be studied in detail in [31].

In the specific case when $\theta_i = \pi/2$, this Wilson loop preserves 1/4 of the supersymmetries of the theory, fitting a general ansatz for supersymmetric Wilson loops found by Zarembo [23]. The action for the string solution in this case vanishes, giving the Wilson loop expectation value unity. It was subsequently proven that this Wilson loop is equal to one to all orders in perturbation theory [32, 33].

If $\theta_i = 0$ the surface will stay at the north pole, so the S^5 ansatz is trivial, this is just the AdS_2 solution discussed in section 4.1.

4.3.3 Coincident circles

The most complicated example in this sector is that of two coincident circular loops. The two circles may be oriented in the same way, or in opposite directions, and as above we allow a periodic coupling to the scalars.

The case of oppositely oriented circles is rather subtle. If we considered coincident lines the potential between them would diverge. One way to see that is to consider the solution with the lines separated, where they will exhibit a Coulomb potential, which will diverge when they coincide. The surface describing them will get closer and closer to the boundary and in the limit it becomes singular.

Another way of seeing this is to take the solution for coincident lines (3.59) with $a^2 > 0$. The range of σ is then π/a and has to be equal to that on the sphere, which for the S^2 ansatz (2.16) is

$$\delta\sigma = \frac{\pi}{a} = \frac{1}{a}\left|F\left(\theta_f\middle| i\frac{m}{a}\right) - F\left(\theta_i\middle| i\frac{m}{a}\right)\right|. \tag{4.31}$$

The right-hand satisfies the following inequalities

$$\left|F\left(\theta_f\middle| i\frac{m}{a}\right) - F\left(\theta_i\middle| i\frac{m}{a}\right)\right| \leq 2K\left(i\frac{m}{a}\right) \leq \pi\,, \tag{4.32}$$

where θ_i and θ_f are the boundary values of θ on the two circles. Hence the equation for $\delta\sigma$ can only be satisfied for $\theta_i = 0$ and $\theta_f = \pi$, where this solution is not the dominant one.

The same is true if we take the S^1 ansatz (2.11), where the range of σ is $\delta\sigma = \delta\varphi_1/a$, and again there will be no solution for $\delta\varphi_1 < \pi$. The absence of a regular solution in those examples is an indication of a divergence, at a finite separation there would be a solution but it becomes singular, and the action diverges, as the lines are brought together.

The same should generically be true for coincident circles. This explains why for most of the range of parameters we will not find solutions with finite action. For certain values there are solutions with finite action for this case, but one has to take them with a grain of salt, we do not know if there is another singular contribution. That will require looking at the limit of nearly coincident circles mentioned above.

When the circles are oriented in the same direction there is no such danger, the minimal surface has to cover twice the AdS_2 subspace (for oppositely oriented circles it will cover twice a ring near the boundary of AdS_2). Still we will find nontrivial solutions only for a small range of parameters. The reason is not fully clear to us, but a possible explanation is the following intuition from flat space.

Consider two circles of the same orientation in flat space. Generally there will be only the disconnected solution, two discs. But if the circles are in the same plane and overlapping there is also a connected solution. It will cover the same area as the disconnected one, but the two sheets will connect there to make a single surface. To avoid confusion, the surface that looks like an annulus and doesn't cover the smaller circle is not allowed because of the orientation.

JHEP01(2006)056

From this example we see that in generic situations there will not be connected solutions for loops of the same orientation. In the case of two concentric circles considered in section 4.2, there is no such solution. On the other hand, if the two surfaces of the disconnected solution touch, it's possible to change the topology of the surface there into a connected solution.

This indeed happens in this example. If we consider the disconnected solution and arrange for both parts to wrap the same hemisphere in S^2, at the north pole the surface will be at the same position in AdS_5 (at $r_1 = 0$). So such a connected solution will exist, and will have the same action as the disconnected solution, and if the two circles are on the same hemisphere this is the dominant solution. This solution has $a^2 = 0$, exactly like the disconnected one, but we may try to look for other connected solutions. We did indeed find some such solutions for a certain range of parameters.

Since the coordinate z will not be bound we have to look at the AdS_2 solution (3.44) with $a^2 < 0$, and the S^2 solution (2.18). We looked in detail at the case when $\theta_i = \theta_f$, where the equation for the range of σ is

$$\delta\sigma = \frac{2}{b} K\left(\sqrt{1 - \frac{k^2}{b^2}}\right) = \frac{2}{b} F\left(\arccos \frac{\cos\theta_i}{\cos\theta_m}\middle| i\cot\theta_m\right), \tag{4.33}$$

with $b^2 = -a^2$ and $\sin\theta_m = b/m$.

For $m > k$ there are no solutions to this equation. To see that, note that the right-hand side is not greater than the complete elliptic integral $2K(\sqrt{1 - m^2/b^2})/b$, which for $m > k$ is smaller than the left-hand side. But for all $m < k$ we did find solutions, and the connected solution always has smaller action than the disconnected one.

Let us turn now to the case of circles with opposite orientation, where the minimal surface will not cover the full AdS_2 subspace, but stay near the boundary. That means the coordinate z will have a maximum, which is the case of positive a^2. The solution to the AdS_5 part of the ansatz is given by (3.38) and to the S^5 ansatz is given by (2.15).

The range of the world-sheet coordinate σ will be given by (3.39). This has to equal the range calculated on the S^2 side (2.16), giving the relation

$$\delta\sigma = \frac{2}{a} K\left(i\frac{k}{a}\right) = \frac{1}{a}\left|F\left(\theta_f\middle| i\frac{m}{a}\right) - F\left(\theta_i\middle| i\frac{m}{a}\right)\right|. \tag{4.34}$$

Let us assume without loss of generality that $\theta_i < \theta_f$ and also that $\theta_i < \pi/2$. In the special case that $m = 0$ there is no dependence on φ_1, so the S^5 ansatz reduces to an S^1 and the right hand side becomes $(\theta_f - \theta_i)/a$. This is a limiting case of the system studied in section 4.2 when the two circles are coincident, i.e. $\delta v = 0$. This limit is singular and the action diverges.

In general, since $\theta_f \leq \pi$ and $\theta_i \geq 0$, the right hand side of equation (4.34) will be smaller than twice the complete elliptic integral $2/a\, K(im/a)$. The complete elliptic integral with imaginary modulus is a a monotonously decreasing function from $K(0) = \pi/2$, approaching zero at infinite imaginary modulus. Therefore if $m > k$ the right hand side is smaller than the left hand side for all values of a. Thus there will be no regular connected classical solution.

JHEP01(2006)056

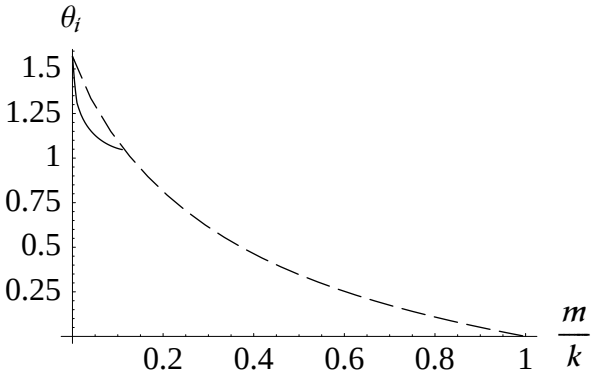

Figure 3: Phase diagram for two coincident circles with rotation on S^2 at angles $\theta_i + \theta_f = \pi$. Regular connected solutions exist only to the left of the dashed line, when $\theta_f - \theta_i$ is not too small, and m/k not too large. The disconnected solution has smaller action in the entire range except for the small region above the solid line.

Hence we should study the existence of solutions for $m < k$. Let us focus on the case where $\theta_f = \pi - \theta_i$, then we use the fact that the elliptic integral with argument θ_i and $\pi - \theta_i$ add up to twice the complete elliptic integral to rewrite (4.34) as

$$F\left(\theta_i \middle| i\frac{m}{a}\right) = K\left(i\frac{m}{a}\right) - K\left(i\frac{k}{a}\right). \tag{4.35}$$

For certain values of θ_i there will be solutions to the equation, and for others not. The solutions will exist for θ_i smaller than a critical value, and will not exist if θ_i exceeds it. We interpret that to mean that when θ_i and θ_f are too close to each other the phenomenon described above happens—the potential between the two circles will diverge.

In all those case there is also a disconnected solution, just two of the surfaces described in the preceding subsection. It turns out that in most of the range where the connected solution exists, the disconnected one has lower action and will dominate. The results of our numerical studies are shown in figure 3. Connected solutions exist to the left of the dashed curve, and they dominate the action only in the small region bound by that curve and the solid line.

4.4 $AdS_3 \times S^3$ subspace

4.4.1 Anti-parallel lines with rotation

We wish to consider here two anti-parallel Wilson loops extended in the x_1 direction, separated by a distance R in the x_2 direction (1.2). Along each of the lines we include in the Wilson loops a coupling to the scalars which is periodic around a circle, that is (1.6) with $\psi = \pi/2$ and only $m = m_1 \neq 0$. So the first line will set the initial conditions

$$x_1 = \tau\,, \qquad x_2 = -\frac{R}{2}\,, \qquad \theta = \theta_i\,, \qquad \varphi_1 = m_i\tau\,, \qquad \varphi_2 = \varphi_{2i}\,. \tag{4.36}$$

Along the second line will set the final values

$$x_1 = \tau\,, \qquad x_2 = \frac{R}{2}\,, \qquad \theta = \theta_f\,, \qquad \varphi_1 = m_f\tau\,, \qquad \varphi_2 = \varphi_{2f}\,. \tag{4.37}$$

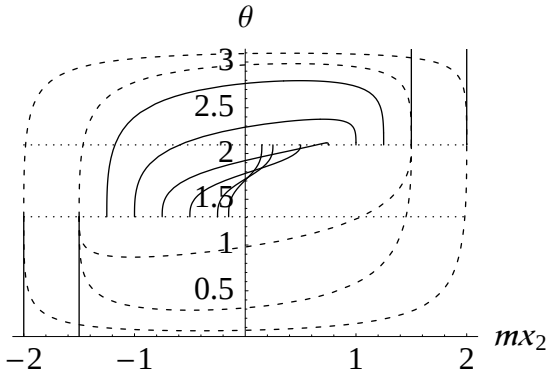

Figure 4: The values of θ as a function of the spatial coordinate x_2 for boundary values $\theta_i = 5\pi/12$ and $\theta_f = 2\pi/3$ (the dotted horizontal lines) and different separation. At very large separation ($mR = 3$, 4) there are connected solutions (dashed) but the disconnected solution (solid) dominates. As shorter separation ($mR = 1.5$, 2, 2.5) the connected solutions dominate and have a turning point $\theta_m > \theta_f$. At shorter distances the solution does not have a turning point.

The S^3 ansatz in section 2.3 allows the two lines to be at different values of φ_2, as indicated above. In the examples we consider below, though, we will take this angle to be a constant, to simplify the expressions, which will then fit the S^2 ansatz in section 2.2.

In the above ansatz we allowed the two lines to rotate with different parameters m. If $m_f = m_i$ the two lines rotate together, while for $m_f = -m_i$, they are rotating in opposite directions. In the former case the angle θ will not have to go through zero. In the latter, since the two rotations have opposite orientation, θ will have to go through zero. In fact, we can consider this case on the same footing as the other by the replacement $m_f \to -m_f$ and $\theta_f \to -\theta_f$. So negative θ correspond to rotation with the opposite orientation.

Another case we may consider is for $m_f = 0$, which is realized by $\theta_f = 0$.

Some of those loops were already studied by Tseytlin and Zarembo [24]. We generalize their solutions and study them further.

As usual, we will have to equate the range of the world-sheet coordinate σ, which for the S^3 ansatz can be found from the expressions in section 2.3. Since we restrict ourselves to the S^2 case we have (2.16) for $a^2 > 0$ and (2.19) for $a^2 < 0$. From the AdS_5 part of the ansatz $\delta\sigma$ is given by (3.55).

Let us first study the case where $m_f = m_i$ (and label it m). The initial and final values θ_i and θ_f are both positive. We found four different types of solutions for these boundary conditions that will be realized for different values of the parameters. We illustrate some of them in figure 4 for $\theta_i = 5\pi/12$ and $\theta_f = 2\pi/3$.

One solution, which exists for all values of the parameters is the disconnected one. It is simply two of the lines considered in section 4.3.1, with action

$$\mathcal{S} = \frac{T\sqrt{\lambda}}{2\pi}\, m(2 - |\cos\theta_i| - |\cos\theta_f|)\,. \tag{4.38}$$

There are also connected solutions for all values of the parameters, but their nature depends on the separation between the lines. When the two lines are very far apart the connected solution will be described by the solution with negative a^2 (2.18) with a turning point θ_m. It will start at θ_i, go to θ_m, near 0 or π and then back to θ_f. For some values there would be only one such solution, and in other cases two or even more (see figure 4).

If the distance between the lines is large enough it's also possible to construct classical solutions that oscillate a few times. They will go to some θ_m, then to $\pi - \theta_m$, and back. Those solutions will never dominate the action.

As the lines get closer, θ_m will approach θ_i or θ_f, and beyond that this branch of the solution will cease to exist. Instead there will be a new solution which still has negative a^2, but will not have a turning point. Those solutions can still be described by some value of θ_m, but it will not be along the world-sheet. As the lines get closer this θ_m will get again closer to 0 or π.

Finally, when θ_m reaches the north or south pole we have to look at solutions with $a = 0$, which are quite easy to study. In this special case the solution to the AdS_5 part is identical to that of the parallel lines with no motion on S^5, studied in [19, 20] and reviewed in section 4.2. The separation between the lines is given by (4.16) as a function of p. The value of p can be found by solving the equation for the range of σ, which using (2.13) is

$$\delta\sigma = \frac{2}{\sqrt{p}} K(i) = \frac{\Gamma(1/4)^2}{2\sqrt{2\pi}} \frac{1}{\sqrt{p}} = \frac{1}{m} \left[\operatorname{arccosh} \frac{1}{\sin\theta_i} + \operatorname{arccosh} \frac{1}{\sin\theta_f} \right]. \tag{4.39}$$

At even closer separation a^2 will be positive and the solution will be described by (2.15).

This suggests a phase diagram with four phases, one where the disconnected solution dominates, and three with connected solutions: Negative a^2 and a turning point, negative a^2 without a turning point and positive a^2. We now turn to study those phases in some specific examples.

Let's start considering the particular case $\theta_i = \theta_f$. In this simple case we find that almost always $a^2 < 0$, and there is a turning point at $\sin\theta_m = b/m$ with $b^2 = -a^2$. In that case we find the relation (2.19), (3.55)

$$\delta\sigma = 2y_+ K\left(ipy_+^2\right) = \frac{2}{b} F\left(\arccos \frac{\cos\theta_i}{\cos\theta_m} \middle| i\cot\theta_m \right). \tag{4.40}$$

with (3.53)

$$y_+^2 = \frac{b^2 + \sqrt{b^4 + 4p^2}}{2p^2}. \tag{4.41}$$

For $\theta_i < \pi/2$ we can always find a solution to these equations. The further the two lines are from each other the smaller $\sin\theta_m$ would be, and as they get closer θ_m approaches the initial value θ_i. In the special case of $\theta_i = \pi/2$, were the initial and final positions are along the equator of S^2 the solution ceases to exist for $mR \lesssim 2.312$. At shorter distances we have to use the other solution discussed at the end of section 2.2, where $\theta_m = \pi/2$. Without the AdS_5 contribution this solution would be unstable, but here it is in fact realized. The transition between those two solutions was explained in [24], which studied exactly this system with $\theta_i = \theta_f = \pi/2$.

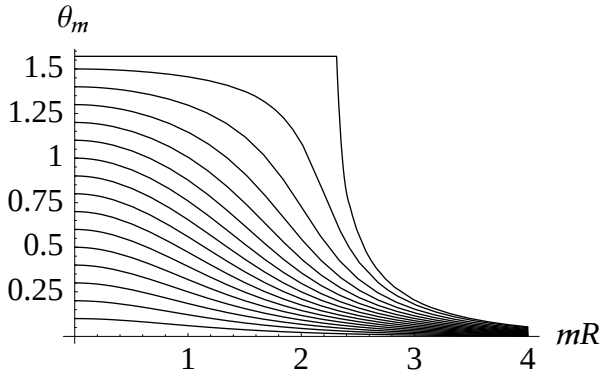

Figure 5: θ_m, the minimal value of θ for two lines separated a distance R with wrapping m times around the sphere. The initial and final values of θ (which are equal in this case) can be read from the intersect of the lines with the axis at $R = 0$, since then $\theta_m = \theta_i$. The bend in the curve gets sharper the larger $\sin\theta_i$ is, and for $\theta_i = \pi/2$ it is not differentiable.

We illustrate this behavior in figure 5, where we plot the value of the turning point θ_m as a function of the distance between the lines (multiplied by the rotation parameter m, to make it scale invariant) for different values of θ_i. As $mR \to 0$ the turning point approaches θ_i, and it gets closer to the pole as mR is increased. In the special case of $\theta_i = \pi/2$ the curve is non-differentiable, due to the phase transition between the two solutions. For all other values of θ_i the curve is smooth, but the bend gets sharper as we approach $\theta_i = \pi/2$.

The action for this solution is given by the sum of the S^2 contribution (2.20) and that of AdS_5 (3.58). It is always smaller than that of the disconnected solution.

Another example where the expressions are simple, but the phase structure much richer is for $\theta_f = \pi - \theta_i$. At very large separation the disconnected solution will always dominate, the two pieces will cover parts of the two hemispheres, and will not cross $\theta = \pi/2$ as the connected solution has to. The action is (2.14)

$$\mathcal{S} = \frac{T\sqrt{\lambda}}{2\pi}\, 2m(1 - |\cos\theta_i|)\,. \tag{4.42}$$

This solution will coexist with the connected solutions and dominate at large distances. There will be a first order phase transition when the connected solutions start dominating. Figure 6 shows the different phases for those boundary values, the disconnected solutions dominate everywhere to the right of the solid line.

For large separation R the connected solution that is realized is the one with a turning point at $\sin\theta_m = b/m$. Since θ_i and θ_f are complementary the sum of the two elliptic integrals in (2.19) is the complete integral. Combining with (3.55) we get the relation

$$\delta\sigma = 2y_+\, K\left(ipy_+^2\right) = \frac{2}{b}\, K\left(i\cot\theta_m\right), \tag{4.43}$$

where y_+ is like in the previous example. Note that this equation is independent of the value of θ_i, and is identical to the equation in the last example (4.40) for the case of $\theta_i = \theta_f = \pi/2$.

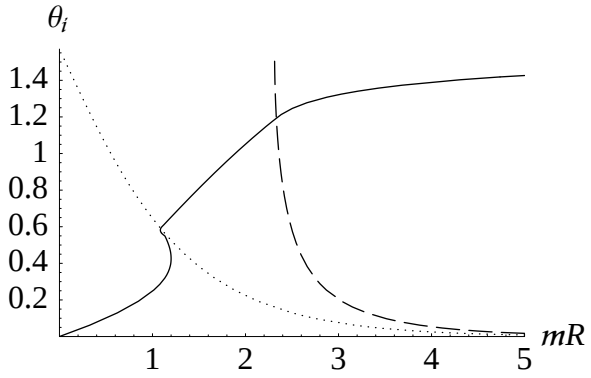

Figure 6: The phase diagram for two lines wrapping the sphere at angles $\theta_i + \theta_f = \pi$. For all values of θ_i and R there are at least two solutions, including one disconnected and one connected. The disconnected solution has lower action to the right of the solid curve, and the connected ones to the left. The connected solution has positive a^2 to the left of the dotted curve (given by (4.45)) Between the dotted and dashed curve the solution has negative a^2, but no turning point. And to the right of the dashed line the solution has a turning point. The solid line and dotted one seem to represent first order phase transitions, and the dashed one a second order one.

This equation can always be solved, but the solution may have $\sin\theta_m = b/m > \sin\theta_i$, which is unphysical. The value of θ_m as a function of mR is the uppermost curve in figure 5. In the present case this phase ceases to exist for $\theta_i = \theta_m$. Therefore this same curve serves now as the phase boundary and is illustrated by the dashed line in figure 6.

Beyond that point the connected solution will still have negative a^2, but there will not be a turning point. It will be described by the (2.18) with only the positive branch and the negative signs in (2.19) and (2.20). The range of σ is

$$\delta\sigma = 2y_+ K\left(ipy_+^2\right) = \frac{2}{b}\left[K\left(i\cot\theta_m\right) - F\left(\arccos\frac{\cos\theta_i}{\cos\theta_m}\middle| i\cot\theta_m\right)\right]. \tag{4.44}$$

The action for this solution is given by the usual expressions. It is interesting to look at it close to the transition to the phase discussed before. From the numerical data it seems like the phase transition is of second order.

As the separation R is decreased we find that $b \to 0$, which happens at a value of p given by (4.39). Combining that with (4.16) we find the relation between R and θ_i to be

$$\cosh\left(\frac{\Gamma(1/4)^4}{16\pi^2}mR\right) = \frac{1}{\sin\theta_i}. \tag{4.45}$$

This relation is shown by the dotted line in figure 6.

At shorter separations the connected solution will have positive a^2. Numerical analysis suggests the phase transition between negative and positive a^2 is of first order.

Note that for the special case of $\theta_i = 0$ and $\theta_f = \pi$ the string starts at the north pole and ends at the south pole. In this case m plays no role at the boundary. In fact this configuration has the same boundary conditions as for two lines in the $AdS_3 \times S^1$ ansatz separated by an angle $\delta\varphi = \pi$. In section 4.2 we saw that in this case there was

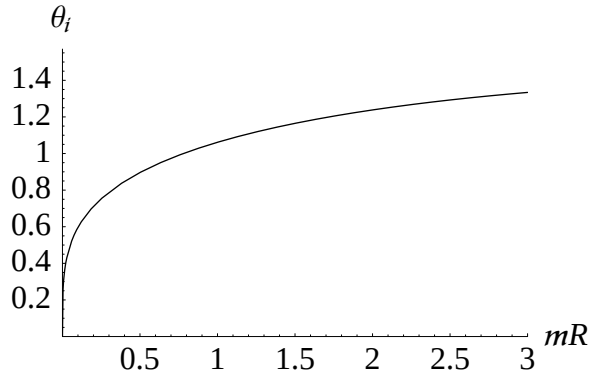

Figure 7: The phase diagram for two lines with rotations in opposite directions at angles $\theta_f = \theta_i - \pi$. For all values of the separation R there are connected solutions with $a^2 > 0$, but to the right of the curve the disconnected solution dominates.

no connected solution. Allowing for the S^2 ansatz here, we do find a connected solution, but its action is greater than the disconnected one for all separations (the bottom of figure 6).

Let us now leave this case and look briefly at some examples with $m_f = -m_i$. It is simpler, as explained above, to describe them by allowing negative θ, so we take positive θ_i and negative θ_f and replace $m_f = m_i = m$.

In this case there seem to be only two phases, the connected solution with $a^2 > 0$ and a disconnected one. The disconnected one will not be dominant unless θ_i and θ_f are on different hemispheres.

Thus an interesting case is the one with $\theta_f = \theta_i - \pi$ (or alternatively $\theta_f = \pi - \theta_i$ and $m_f = -m_i$). The connected solution has $a^2 > 0$, and again the sum of the two elliptic integrals is the complete integral

$$\delta\sigma = 2y_+ K\left(ipy_+^2\right) = \frac{2}{a} K\left(i\frac{m}{a}\right). \tag{4.46}$$

At short distances this connected solution will dominate, but at large distances the action of the disconnected solution, given in (4.42) will be lower. The line separating those two phases is shown in figure 7.

Finally let us comment on the case where $m_f = 0$. That is easy to incorporate into this ansatz by taking $\theta_f = 0$ (or $\theta_f = \pi$). In this case we find a classical solution with $a^2 > 0$ for all values of m and θ_i, and it always has smaller action than the disconnected solution.

4.4.2 Concentric circles with rotation

Another periodic ansatz that fits inside the AdS_3 subspace of AdS_5 is the case of two concentric circles. We now consider this example where the Wilson loop also couples to the scalars in a periodic fashion. The boundary conditions on the first circle are

$$v = v_i = \log R_i\,, \qquad \phi_1 = k\tau\,, \qquad \theta = \theta_i\,, \qquad \varphi_1 = m_i\tau\,, \qquad \varphi_2 = \varphi_{2i}\,. \tag{4.47}$$

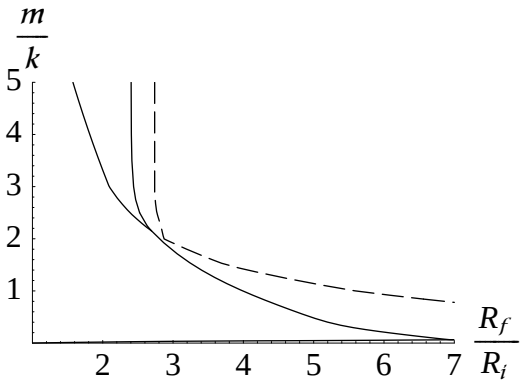

Figure 8: Phase diagram for concentric circles with radii $R_f > R_i$ which rotate k times in $\mathbb{R}^4$ and m times on the sphere with $\theta_i = \theta_f = \pi/2$. The disconnected solution as well as the solution with constant θ exist for all values of the parameters, and in addition there are solutions with a turning point to the left of the dashed line. The solid curve is the phase boundary between that dominated by the disconnected solution (to the right), the connected solution with constant θ (to the left) and the solution with a turning point (above the triple point).

For the second circle we have

$$v = v_i = \log R_i\,, \qquad \phi_1 = k\tau\,, \qquad \theta = \theta_f\,, \qquad \varphi_1 = m_f\tau\,, \qquad \varphi_2 = \varphi_{2f}\,. \tag{4.48}$$

We will not study this general ansatz in detail, there are many parameters to vary and presumably many different phases. We will look only at the case with $\theta_i = \theta_f = \pi/2$, $m_f = m_i = m$ and $\varphi_{2f} = \varphi_{2i}$.

For these values of θ_i and θ_f there are two possible solutions to the S^2 ansatz, that with $-m^2 < a^2 < 0$ (2.18) and the one with $a^2 = -m^2$ mentioned at the end of section 2.2 (and was realized also in the last subsection).

For the case when $a^2 < 0$, the equations for the range of σ are (2.19), (3.20)

$$\delta\sigma = \frac{2z_+}{k} K\left(\frac{z_+}{z_-}\right) = \frac{2}{b}\, K\left(i\cot\theta_m\right). \tag{4.49}$$

with $b^2 = -a^2$ and (3.18)

$$z_\pm^2 = \frac{b^2 + k^2 \pm \sqrt{(b^2-k^2)^2 + 4k^2p^2}}{2(p^2-b^2)}\,, \tag{4.50}$$

The results of the numerical studies are shown in figure 8. This figure is for $R_f > R_i$, and can be extended by the replacement $R_f \leftrightarrow R_i$. For all values of m, k, R_f and R_i both the disconnected solution and the connected one with constant $\theta = \pi/2$ exist. The disconnected one dominates for large values of the ratio R_f/R_i, to the right of the solid curve. What is not obvious from the picture is that R_f/R_i has a maximum of roughly 6.9914 at small m/k and beyond that the curve goes to $R_f/R_i = 1$ at $m/k = 0$.

The solution with negative a^2 exists to the left of the dashed line and dominates the action above the triple point (note that while the dashed line gets very close to the solid one, they do not touch). For very large m/k the leftmost solid line approaches 1, so the unstable solution does not dominate there. The other two lines approach the values 2.4034 and 2.7245, which are the same as the intercept of the lines with the horizontal axis in figure 2. That was the case of two concentric circles with no motion on the S^5 (also studied by [21, 22]).

5. Discussion

The purpose of this article is twofold; to point out that the integrability of the σ-model on $AdS_5 \times S^5$ can be used to calculate Wilson loops within the AdS/CFT correspondence, and to demonstrate this in some specific examples.

It is very easy to integrate the equations of motion, as we did in sections 2 and 3. The results are given by trigonometric and hyperbolic functions as well as elliptic integrals, and more complicated cases would be expressed in terms of hyperelliptic integrals. On the other hand, combining the solutions into full-fledged examples leads to very complex phenomena. There are many solutions to the equations of motion for the same boundary conditions and it requires careful study to find which will dominate.

Some of the solutions exist only for a certain range of parameters, like the catenoid discussed in [30, 21, 22]. Other solutions may coexist for the entire range of parameters (like the connected and disconnected solutions for anti-parallel lines with rotation), with one dominating in a certain regime, and the other in another.

Thus the equations of motion are easy to solve, but fixing the boundary conditions leads to the complicated phase structure. This, in fact, is not unlike the classical problem of soap films in flat space ("Plateau's problem"). The difficulty is not with solving the equations of motion locally, but with satisfying the boundary conditions. These complications raise some questions we would like to discuss now.

Some recent studied of local operators in $\mathcal{N} = 4$ supersymmetric Yang-Mills seem to indicate that in the planar limit the theory is integrable. The integrable structure was found both on the field theory side at weak coupling and in $AdS_5 \times S^5$, corresponding to large 't Hooft coupling. In fact, integrability in this limit is based exactly on the same integrals of motion considered here for the Wilson loop operators.

If the full planar theory is to be integrable, it should include also the Wilson loop operators. As stated, the equations of motion are integrable, which agrees with those expectations, but the existence of multiple solutions complicates matters and is a question that will have to be addressed in making the claim that the planar theory is integrable.

Many confusing issues arise when trying to compare what is known about the integrability of local operators to Wilson loops. Are the basic objects the one-point functions of those operators, or the correlators of two? What is the meaning of the different phase transitions, where the correlator of two loops changes markedly as the boundary conditions are modified.

JHEP01(2006)056

To gain further intuition into those problems it is useful to find some simple operators that can be used as starting points in this investigation. Here we tried to classify the loops according to subspaces they reside within. Clearly the simplest is the circle or line, which live inside an AdS_2 subspace of $AdS_5 \times S^5$. The next level of complication comes from extending it either to $AdS_3 \times S^1$ or to $AdS_2 \times S^2$. Beyond that we considered the case of $AdS_3 \times S^3$.

This classification has some resemblance to the subsectors of local operators related to different spin-chains. The Wilson loops whose minimal surface fit within the $AdS_3 \times S^1$ include two components of the gauge field and two real scalars. That is reminiscent of the spin-chain with one complex scalar and a chiral combination of covariant derivatives. The operators described within $AdS_2 \times S^2$ have a single gauge field and three scalars, which can also be combined into a complex scalar and a chiral operator made of a covariant derivative and scalar. Finally the $AdS_3 \times S^3$ subspace is related to operators with two covariant derivatives and four real scalars, which again has some similarity to the sector of local operators made of two complex scalars and a chiral covariant derivative.

In this paper we studied Wilson loops only in $AdS_5 \times S^5$, and did not touch at all on the gauge theory side of the duality. While the periodic ansatze led to simple equations for the string surface which we solved, the perturbative calculation seems quite complicated. We did not find analogous signs of integrable structure in the weakly coupled field theory.

There are also some conceptual problems that have to be addressed in this comparison. In $AdS_5 \times S^5$ one can consider operators that are localized at the same point on the boundary of AdS_5 but separated only in the S^5 direction. For example, in the example of the single circle in section 4.3.2 we considered the circle wrapping the curve in space k times while wrapping a circle in S^5 m times. There is a nice minimal surfaces with finite action for all integers values of k and m. If one looks at the same Wilson loop operator in the gauge theory, there will be singular graphs that connect different points along the loop that are coincident in space. Those graphs will lead to divergences unless m is divisible by k.

A more extreme example of this is for coincident circles (see section 4.3.3), where for certain values of the parameters we found finite action solutions. Calculating those Wilson loops in perturbation theory involves extremely divergent graphs.

This issue has some similarities to the question of zig-zag symmetry. We know that a Wilson loop does not change under arbitrary reparametrizations, including backtracking. But looking at the part of the loop that backtracks naively in perturbation theory gives a very bad divergence. The coincident circles resemble a backtracking curve, only with different couplings to the scalars, and to capture them requires some regularization that satisfies this general form of zig-zag symmetry allowing for extra motion on S^5.

Another difference between the string theory calculation and that on the gauge theory side is that in the gauge theory at weak coupling there is no sign of those complicated phases we find for the minimal surfaces. This is a phenomenon that must show up only at the level of classical string theory, but the phase transitions should be smoothed out by quantum corrections to the σ-model, and are hard to see from the gauge theory side.

JHEP01(2006)056

There actually is an example of a class of operators where by summing the perturbative result and expressing the results in a $1/\sqrt{\lambda}$ expansion, one finds two saddle points that agree with two solutions found in string theory [31].

Acknowledgments

We would like to thank Gordon Semenoff and Matthias Staudacher for useful discussions. N.D. would like to thank the Weizmann institute, where this project was initiated, for its hospitality. The authors would like to thank the Aspen Center for physics for providing the opportunity to continue this collaboration in an inspiring atmosphere.

References

[1] J.M. Maldacena, *The large-N limit of superconformal field theories and supergravity*, *Adv. Theor. Math. Phys.* **2** (1998) 231 [hep-th/9711200].

[2] N. Beisert, *The dilatation operator of $N = 4$ super Yang-Mills theory and integrability*, *Phys. Rept.* **405** (2005) 1 [hep-th/0407277].

[3] K. Pohlmeyer, *Integrable hamiltonian systems and interactions through quadratic constraints*, *Commun. Math. Phys.* **46** (1976) 207;
M. Lüscher and K. Pohlmeyer, *Scattering of massless lumps and nonlocal charges in the two-dimensional classical nonlinear sigma model*, *Nucl. Phys.* **B 137** (1978) 46.

[4] R.R. Metsaev and A.A. Tseytlin, *Type IIB superstring action in $AdS_5 \times S^5$ background*, *Nucl. Phys.* **B 533** (1998) 109 [hep-th/9805028].

[5] G. Mandal, N.V. Suryanarayana and S.R. Wadia, *Aspects of semiclassical strings in AdS_5*, *Phys. Lett.* **B 543** (2002) 81 [hep-th/0206103].

[6] I. Bena, J. Polchinski and R. Roiban, *Hidden symmetries of the $AdS_5 \times S^5$ superstring*, *Phys. Rev.* **D 69** (2004) 046002 [hep-th/0305116].

[7] S.S. Gubser, I.R. Klebanov and A.M. Polyakov, *A semi-classical limit of the gauge/string correspondence*, *Nucl. Phys.* **B 636** (2002) 99 [hep-th/0204051].

[8] S. Frolov and A.A. Tseytlin, *Semiclassical quantization of rotating superstring in $AdS_5 \times S^5$*, *JHEP* **06** (2002) 007 [hep-th/0204226].

[9] G. Arutyunov, S. Frolov, J. Russo and A.A. Tseytlin, *Spinning strings in $AdS_5 \times S^5$ and integrable systems*, *Nucl. Phys.* **B 671** (2003) 3 [hep-th/0307191].

[10] G. Arutyunov, J. Russo and A.A. Tseytlin, *Spinning strings in $AdS_5 \times S^5$: new integrable system relations*, *Phys. Rev.* **D 69** (2004) 086009 [hep-th/0311004].

[11] J.A. Minahan and K. Zarembo, *The bethe-ansatz for $N = 4$ super Yang-Mills*, *JHEP* **03** (2003) 013 [hep-th/0212208].

[12] D. Berenstein, R. Corrado, W. Fischler and J.M. Maldacena, *The operator product expansion for wilson loops and surfaces in the large-N limit*, *Phys. Rev.* **D 59** (1999) 105023 [hep-th/9809188].

[13] N. Drukker, D.J. Gross and H. Ooguri, *Wilson loops and minimal surfaces*, *Phys. Rev.* **D 60** (1999) 125006 [hep-th/9904191].

JHEP01(2006)056

[14] J.K. Erickson, G.W. Semenoff and K. Zarembo, *Wilson loops in $N = 4$ supersymmetric Yang-Mills theory*, *Nucl. Phys.* **B 582** (2000) 155 [hep-th/0003055].

[15] N. Drukker and D.J. Gross, *An exact prediction of $N = 4$ SUSY M-theory for string theory*, *J. Math. Phys.* **42** (2001) 2896 [hep-th/0010274].

[16] N. Drukker and B. Fiol, *All-genus calculation of wilson loops using D-branes*, *JHEP* **02** (2005) 010 [hep-th/0501109].

[17] G.W. Semenoff and K. Zarembo, *More exact predictions of SUSY for string theory*, *Nucl. Phys.* **B 616** (2001) 34 [hep-th/0106015].

[18] K. Zarembo, *Open string fluctuations in $AdS_5 \times S^5$ and operators with large R charge*, *Phys. Rev.* **D 66** (2002) 105021 [hep-th/0209095].

[19] S.J. Rey and J.-T. Yee, *Macroscopic strings as heavy quarks in large-N gauge theory and anti-de Sitter supergravity*, *Eur. Phys. J.* **C 22** (2001) 379 [hep-th/9803001].

[20] J.M. Maldacena, *Wilson loops in large-N field theories*, *Phys. Rev. Lett.* **80** (1998) 4859 [hep-th/9803002].

[21] K. Zarembo, *Wilson loop correlator in the AdS/CFT correspondence*, *Phys. Lett.* **B 459** (1999) 527 [hep-th/9904149].

[22] P. Olesen and K. Zarembo, *Phase transition in wilson loop correlator from AdS/CFT correspondence*, hep-th/0009210.

[23] K. Zarembo, *Supersymmetric Wilson loops*, *Nucl. Phys.* **B 643** (2002) 157 [hep-th/0205160].

[24] A.A. Tseytlin and K. Zarembo, *Wilson loops in $N = 4$ SYM theory: rotation in S^5*, *Phys. Rev.* **D 66** (2002) 125010 [hep-th/0207241].

[25] A.A. Tseytlin, *Spinning strings and AdS/CFT duality*, hep-th/0311139.

[26] O. Babelon and M. Talon, *Separation of variables for the classical and quantum neumann model*, *Nucl. Phys.* **B 379** (1992) 321 [hep-th/9201035].

[27] A. Mikhailov, *Special contact Wilson loops*, hep-th/0211229.

[28] M. Bianchi, M.B. Green and S. Kovacs, *Instanton corrections to circular wilson loops in $N = 4$ supersymmetric Yang-Mills*, *JHEP* **04** (2002) 040 [hep-th/0202003].

[29] M. Staudacher and W. Krauth, *Two-dimensional QCD in the Wu-Mandelstam-Leibbrandt prescription*, *Phys. Rev.* **D 57** (1998) 2456 [hep-th/9709101].

[30] D.J. Gross and H. Ooguri, *Aspects of large-N gauge theory dynamics as seen by string theory*, *Phys. Rev.* **D 58** (1998) 106002 [hep-th/9805129].

[31] N. Drukker and B. Fiol, in preparation.

[32] Z. Guralnik and B. Kulik, *Properties of chiral Wilson loops*, *JHEP* **01** (2004) 065 [hep-th/0309118].

[33] Z. Guralnik, S. Kovacs and B. Kulik, *Less is more: non-renormalization theorems from lower dimensional superspace*, *Int. J. Mod. Phys.* **A 20** (2005) 4546 [hep-th/0409091].

JHEP01(2006)056